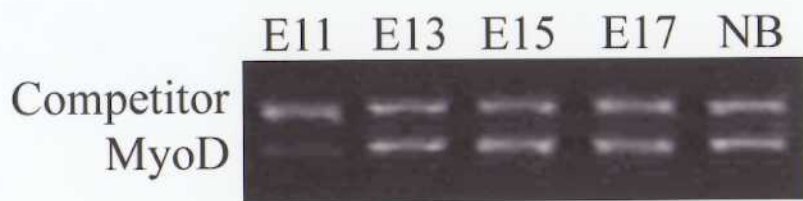


## Figures and Figure Legends

Figure 1.

Electrophoretic gel patterns of myoD and its competitor after competitive-PCR amplification. NB, newborn.



**Figure 2.**

**Changes in the relative amount of desmin mRNA in the mouse tongue and hind limb muscles at stages E11, 13, 15 and 17, and at birth.**

Each point with its vertical bar represents the mean  $\pm$  1 SD of 5 or 6 samples. NB, newborn.

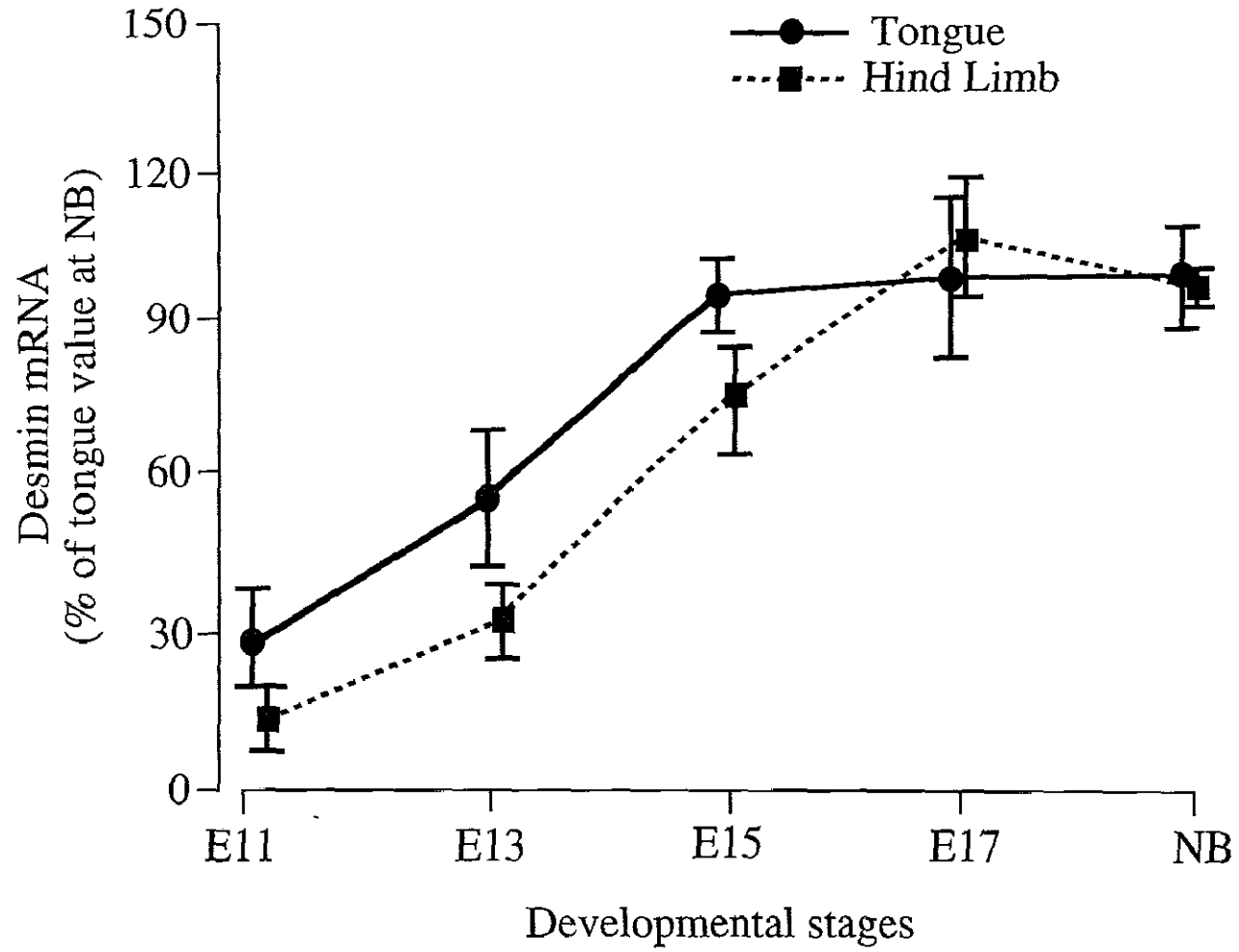


**Figure 3.**

**Changes in the relative amount of muscle creatine kinase mRNA in the mouse tongue and hind limb muscles at stages E11, 13, 15 and 17, and at birth.**

Each point with its vertical bar represents the mean  $\pm$  1 SD of 5 or 6 samples. No muscle creatine kinase mRNA was detected in the tongue and hind limb muscles at E11. NB, newborn. MCK, muscle creatine kinase.

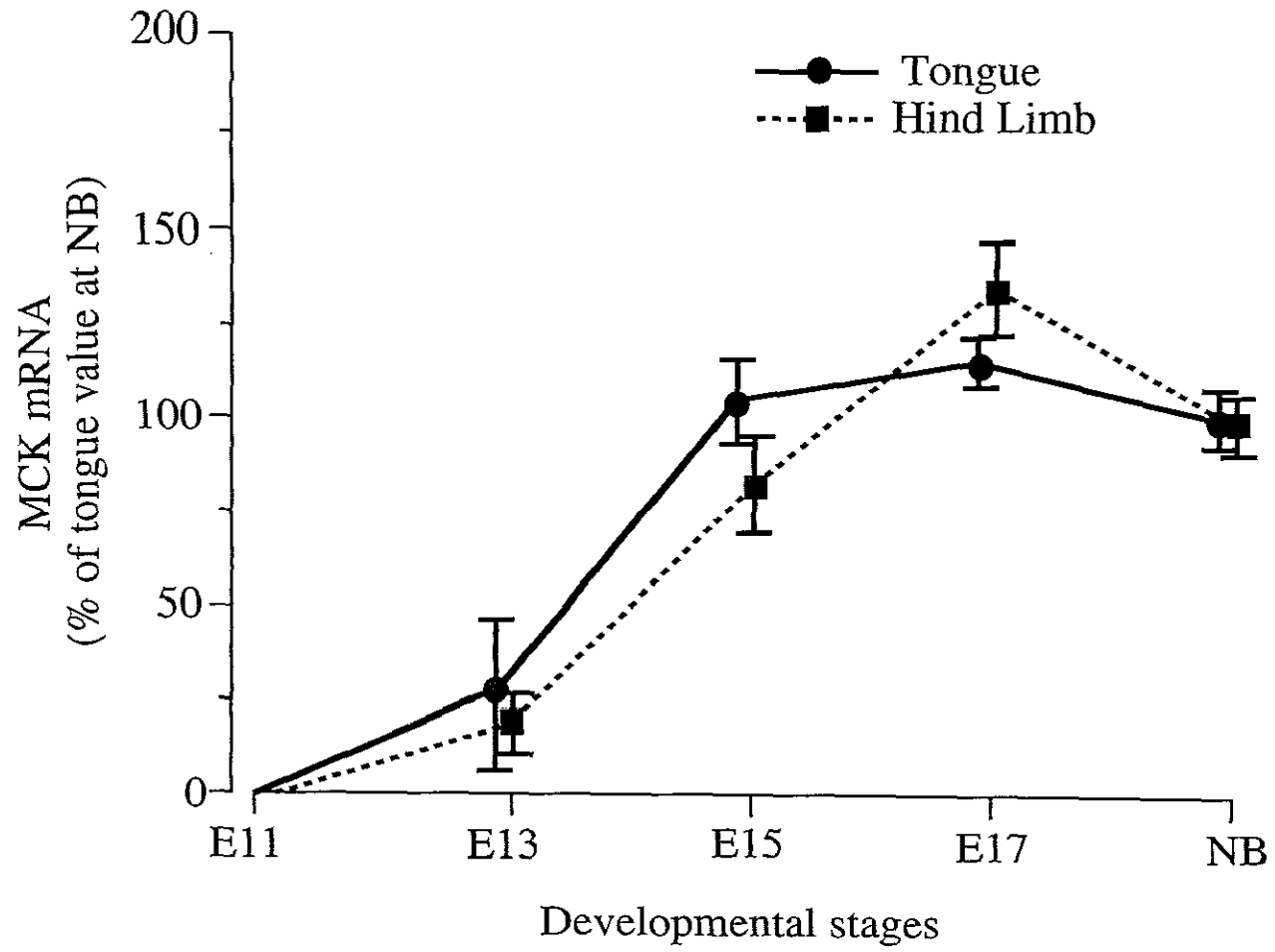


**Figure 4.**

**Changes in the relative amount of fast troponin C mRNA in the mouse tongue and hind limb muscles at stages E11, 13, 15 and 17, and at birth.**

Each point with its vertical bar represents the mean  $\pm$  1 SD of 5 or 6 samples. No fast troponin C mRNA was detected in the tongue and hind limb muscles at E11. NB, newborn. Tn C, troponin C.

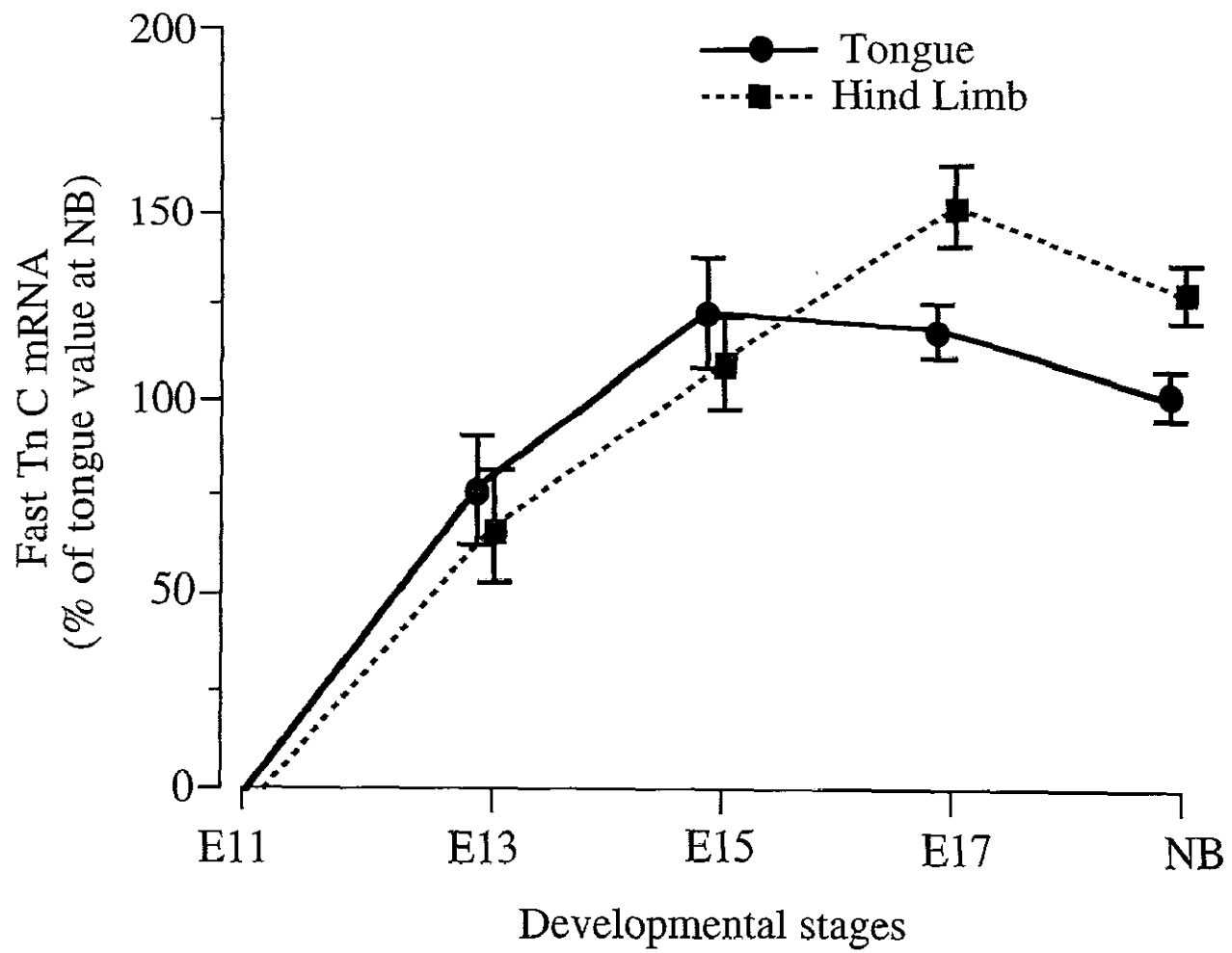


**Figure 5.**

**Changes in the relative amount of slow troponin C mRNA in the mouse tongue and hind limb muscles at stages E11, 13, 15 and 17, and at birth.**

Each point with its vertical bar represents the mean  $\pm$  1 SD of 5 or 6 samples. NB, newborn. Tn C, troponin C.

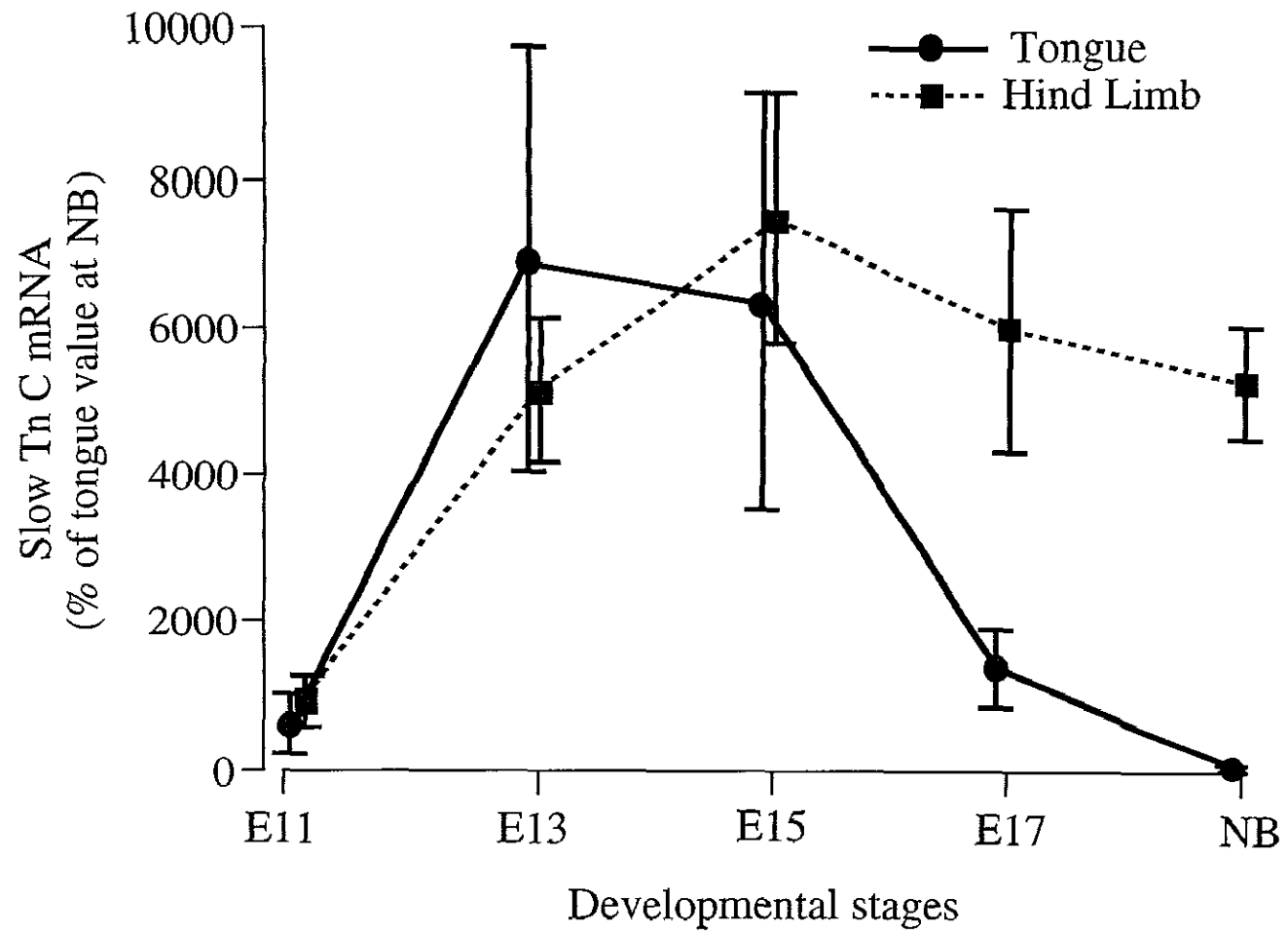
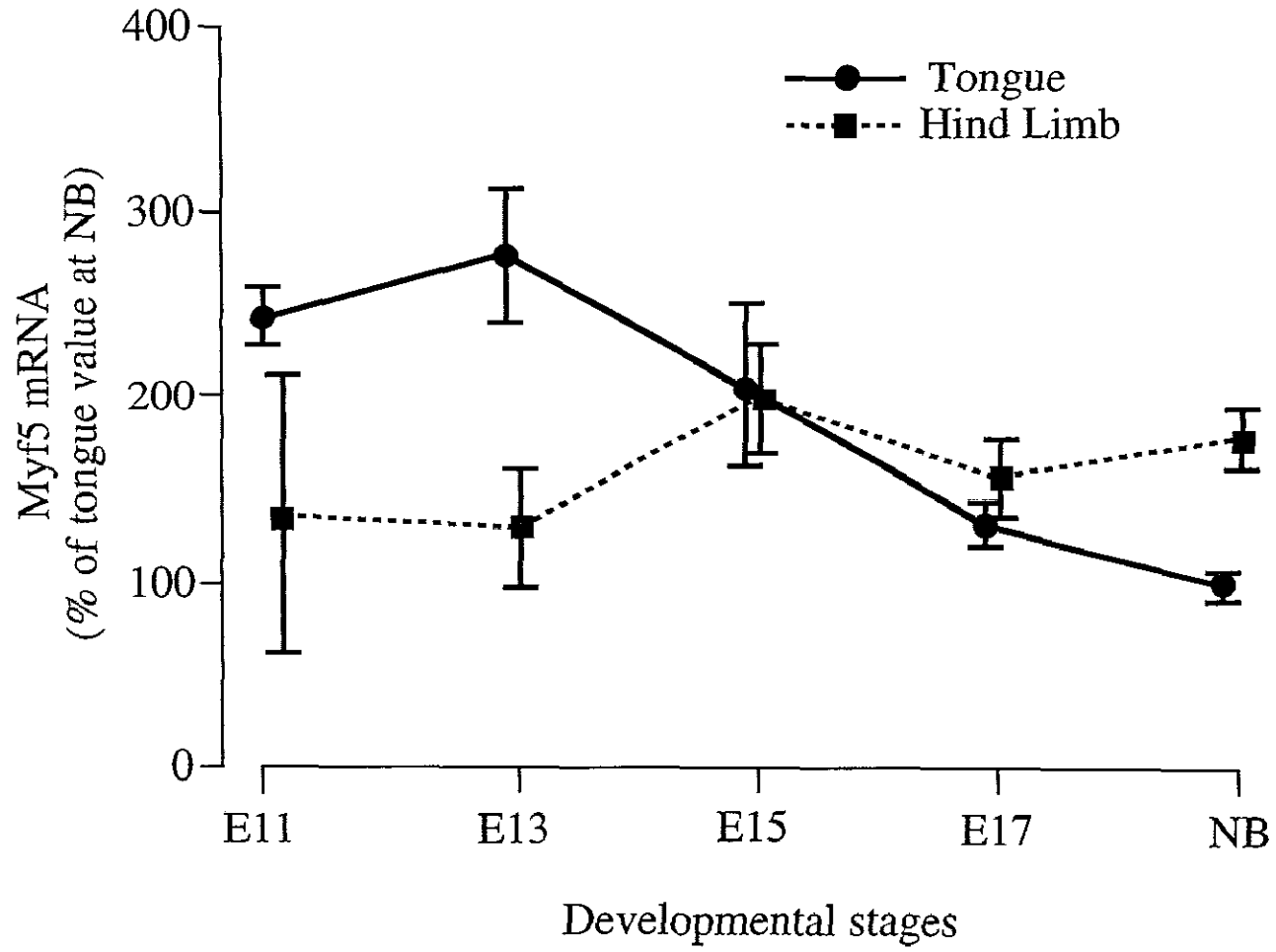


Figure 6.

Changes in the relative amount of myf5 mRNA in the mouse tongue and hind limb muscles at stages E11, 13, 15 and 17, and at birth.

Each point with its vertical bar represents the mean  $\pm$  1 SD of 5 or 6 samples. NB, newborn.



**Figure 7.**

**Changes in the relative amount of myoD mRNA in the mouse tongue and hind limb muscles at stages E11, 13, 15 and 17, and at birth.**

Each point with its vertical bar represents the mean  $\pm$  1 SD of 4 or 6 samples. NB, newborn.

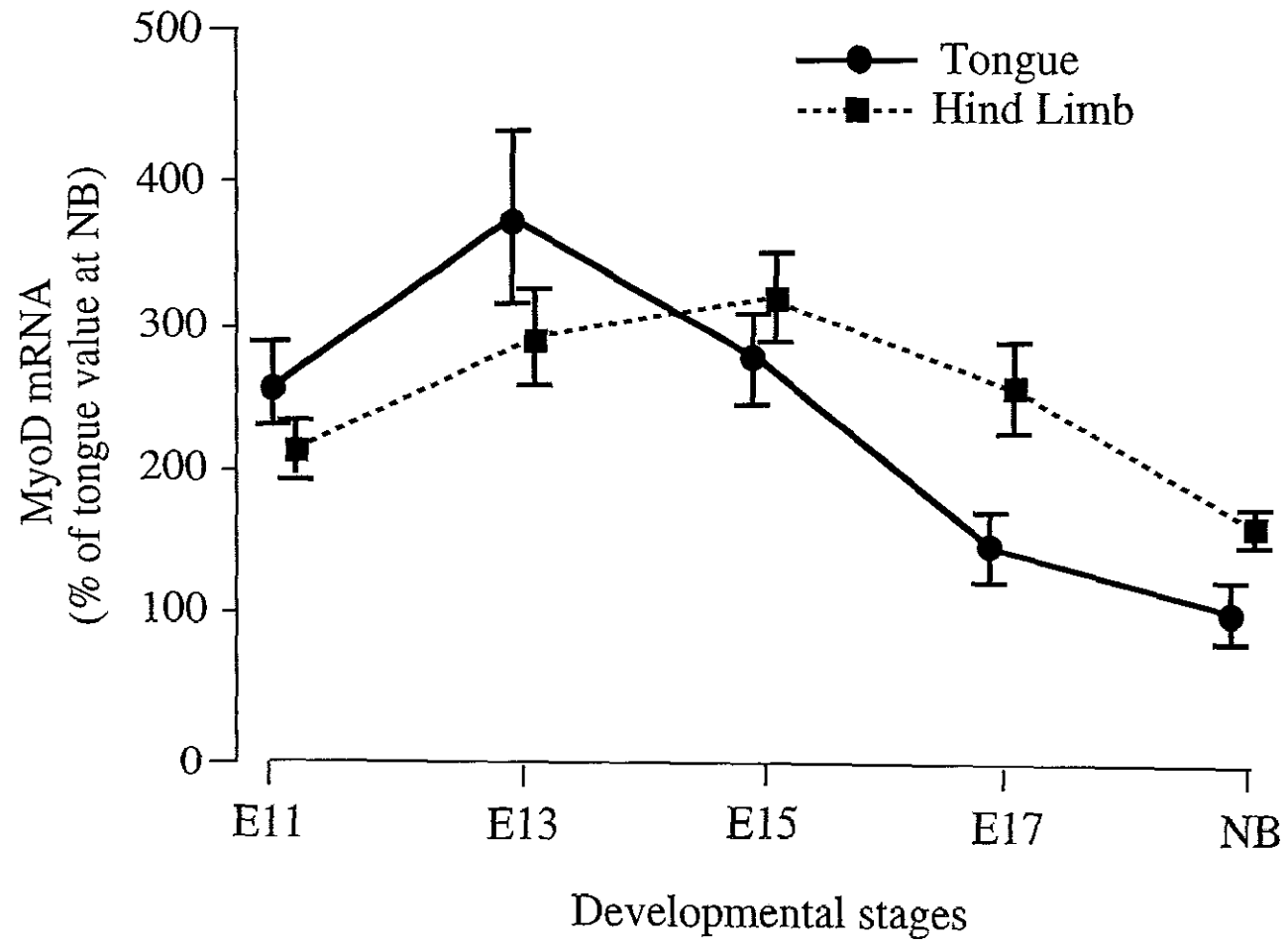
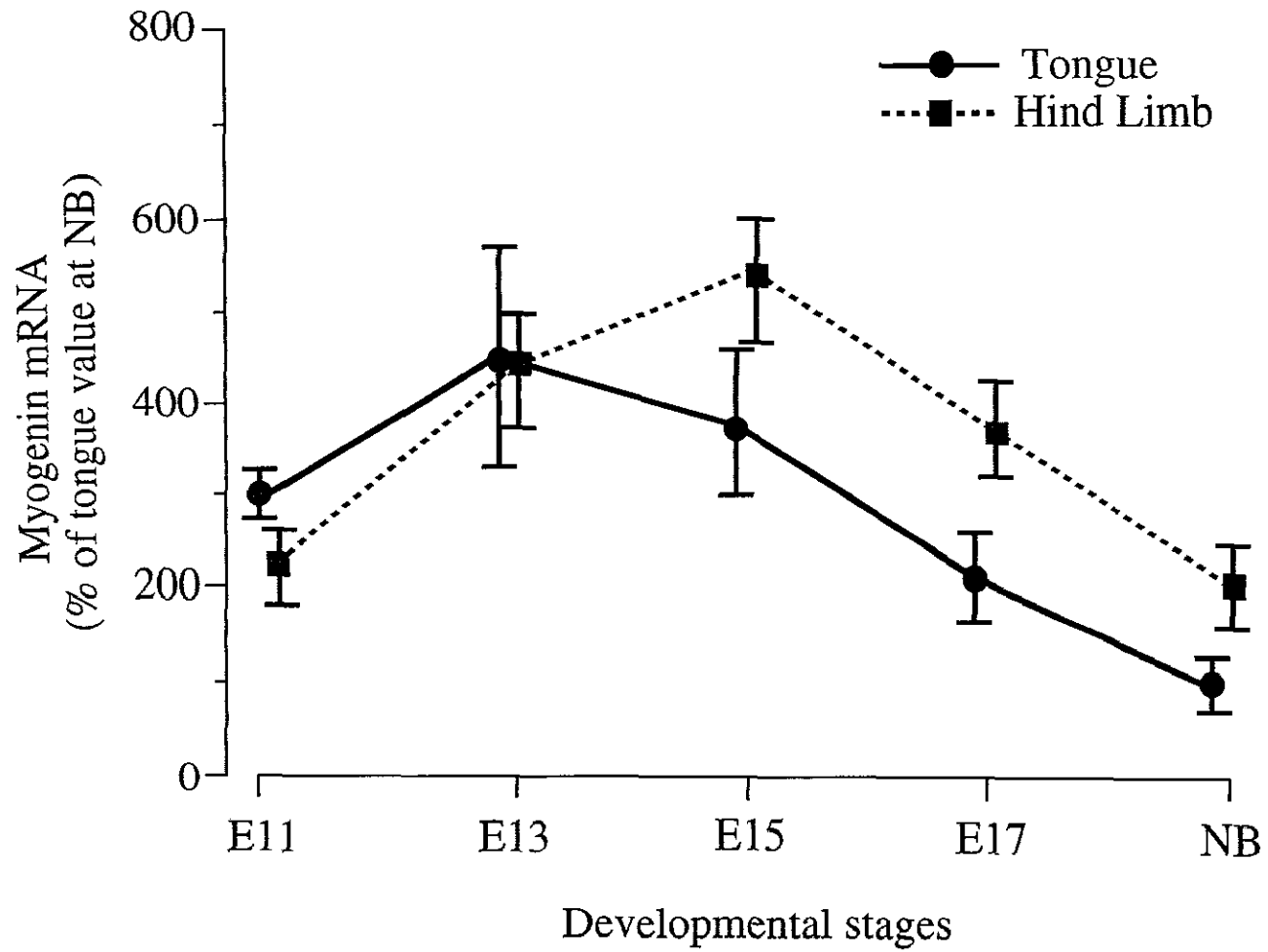


Figure 8.

Changes in the relative amount of myogenin mRNA in the mouse tongue and hind limb muscles at stages E11, 13, 15 and 17, and at birth.

Each point with its vertical bar represents the mean  $\pm$  1 SD of 5 or 6 samples. NB, newborn.



**Figure 9.**

**Changes in the relative amount of MRF4 mRNA in the mouse tongue and hind limb muscles at stages E11, 13, 15 and 17, and at birth.**

Each point with its vertical bar represents the mean  $\pm$  1 SD of 5 or 6 samples. No MRF4 mRNA was detected at E11 in the tongue muscle, and at E11 and 13 in the hind limb muscles. NB, newborn.

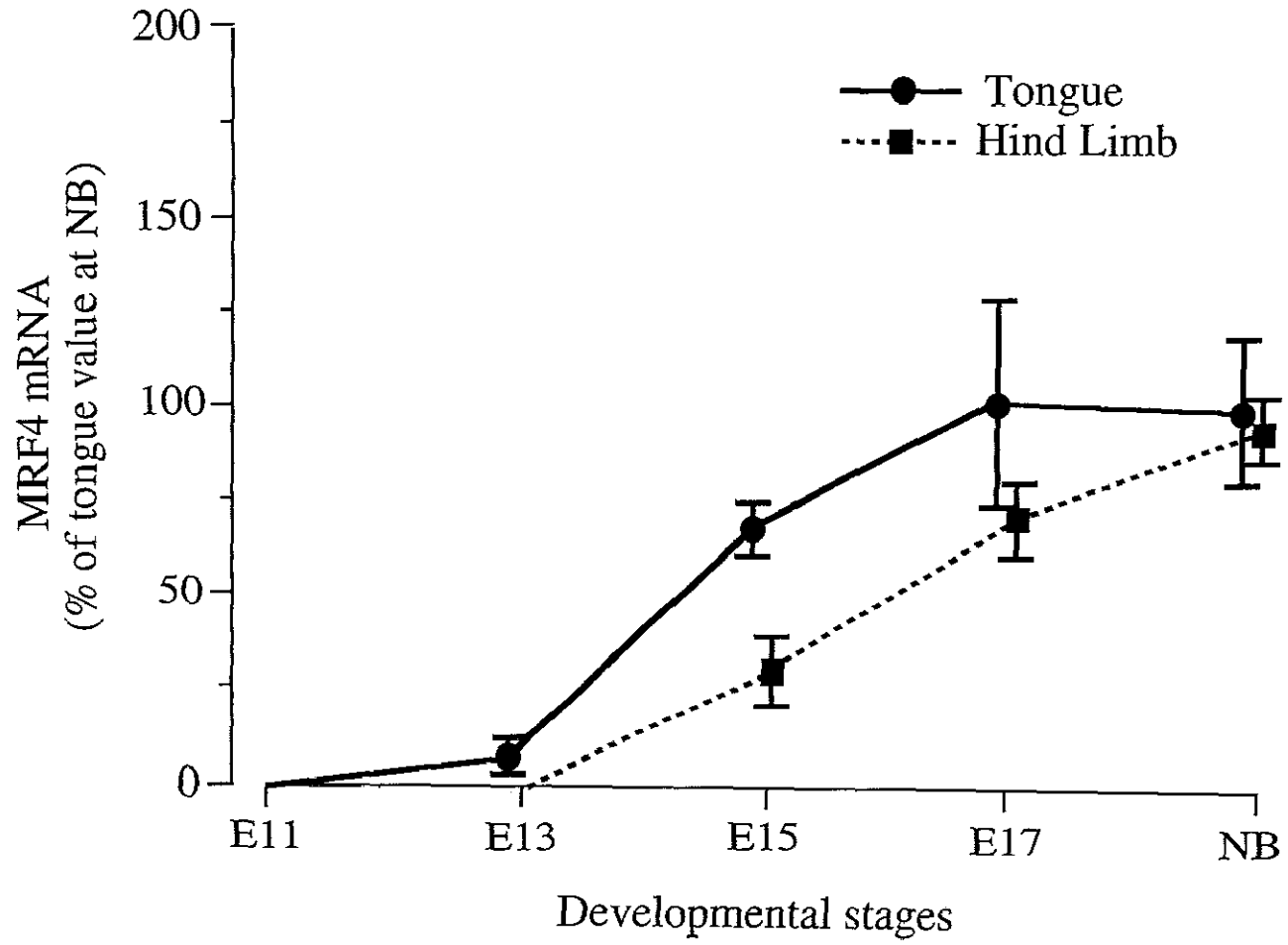


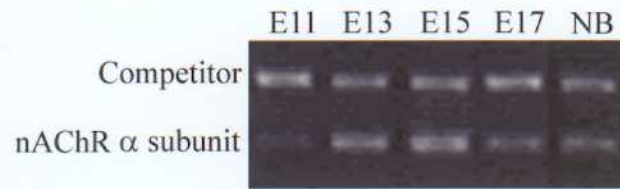
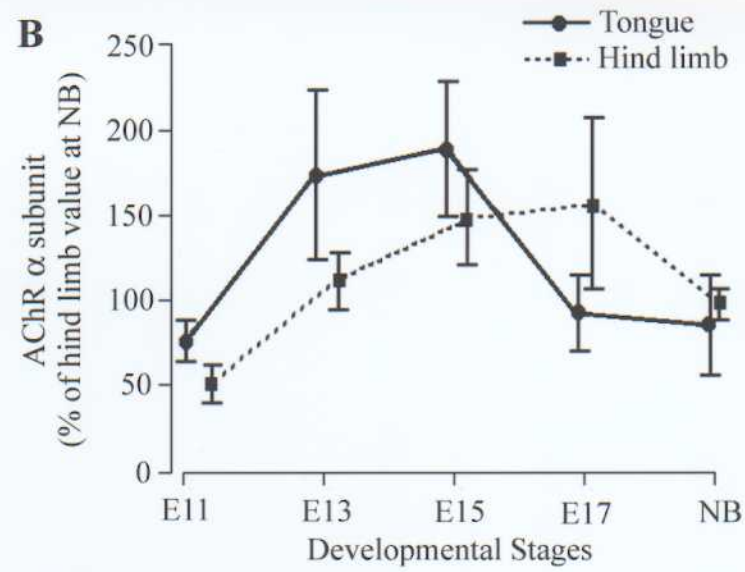
Figure 10.

Electrophoretic gel patterns (A) of the PCR products of the nicotinic acetylcholine receptor (nAChR)  $\alpha$  subunit and its competitor after competitive RT-PCR amplification.

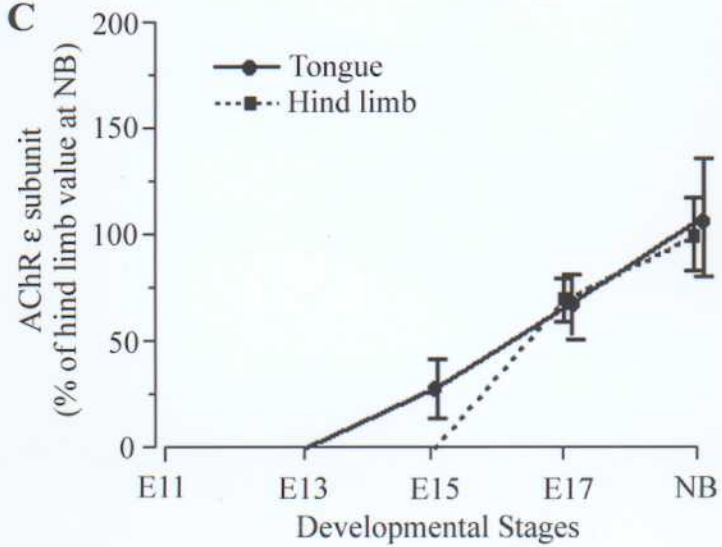
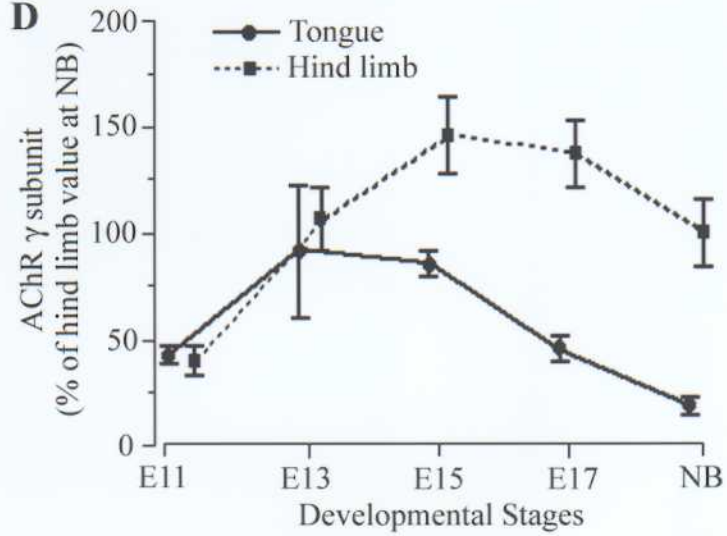
Changes in the relative amounts of the nAChR  $\alpha$  (B),  $\epsilon$  (C) and  $\gamma$  (D) subunits in the mouse tongue and hind limb at stages E11, 13, 15, and 17, and at birth.

Each point and its vertical bar represent the mean  $\pm$  1 SD of five or six samples. The vertical axis is expressed as a percentage of the mean value in the hind limb at birth.

NB, newborn.

**A****B**

96

**C****D**

**Figure 11.**

**Immunolocalization of the nAChR  $\delta$  subunit in the tongue obtained from E13 (A, B), E15 (C, D) and E17 (E, F) mouse embryos, and from newborn mice (G, H).**

The top diagrammatic representation shows a sagittal section of the tongue viewed from the buccal side. The squares in the top diagrammatic representation indicate the regions shown in A ~ H. B ~ F at the same magnification as A. H at the same magnification as G.

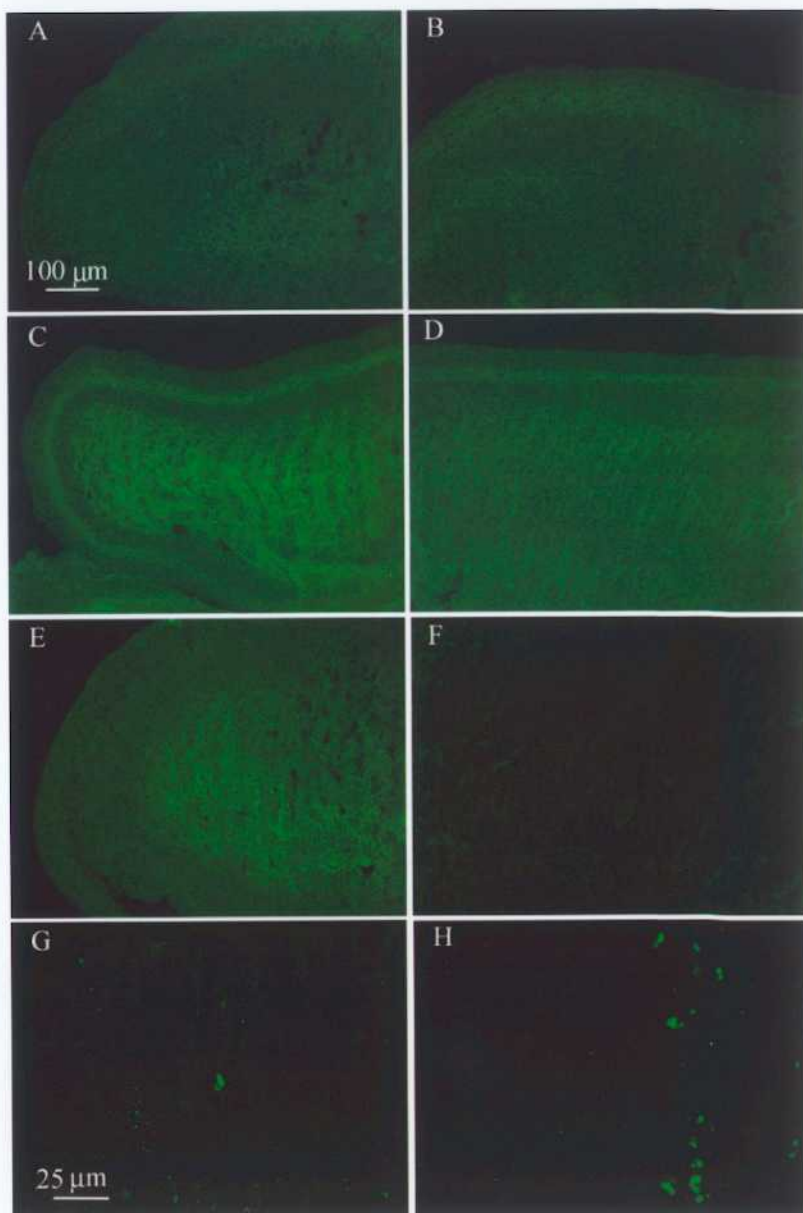
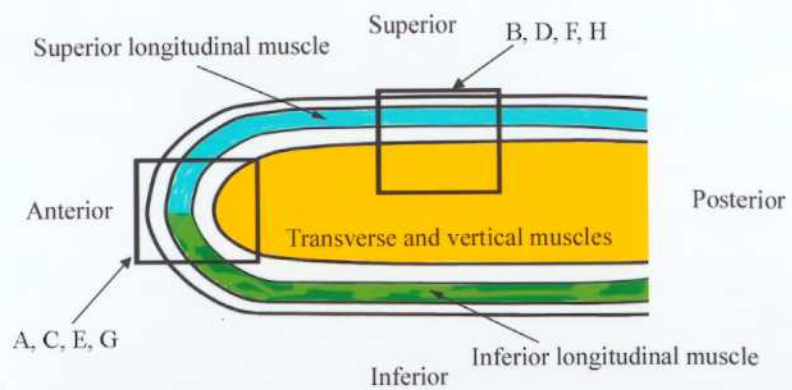
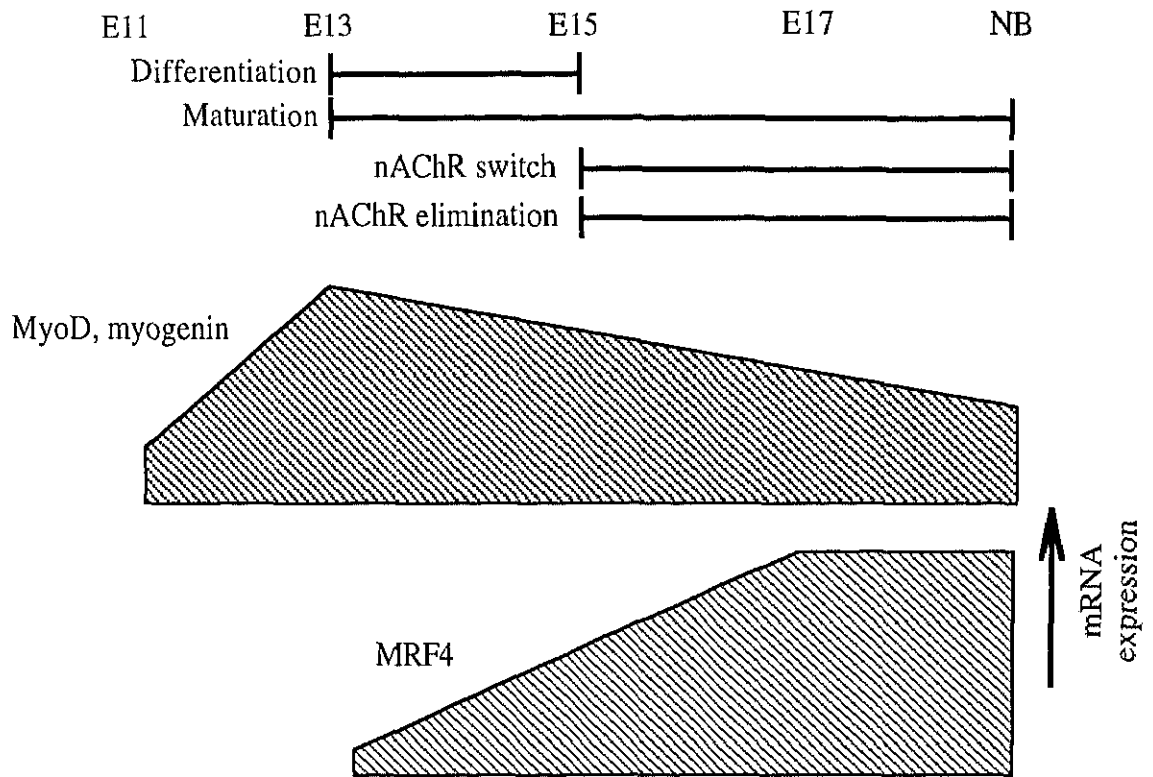


**Figure 12.**

**The synaptogenesis, myogenesis, and the expression of myoD, myogenin, and MRF4 mRNA in the mouse tongue and hind limb.**

Data for the myogenesis and expression of myoD, myogenin, and MRF4 mRNA are from our previous study (Yamane *et al.*, 2000a).

**Myogenesis, Synaptogenesis and myoD family expression in mouse tongue**



**Myogenesis, synaptogenesis and myoD family expression in mouse hind limb**

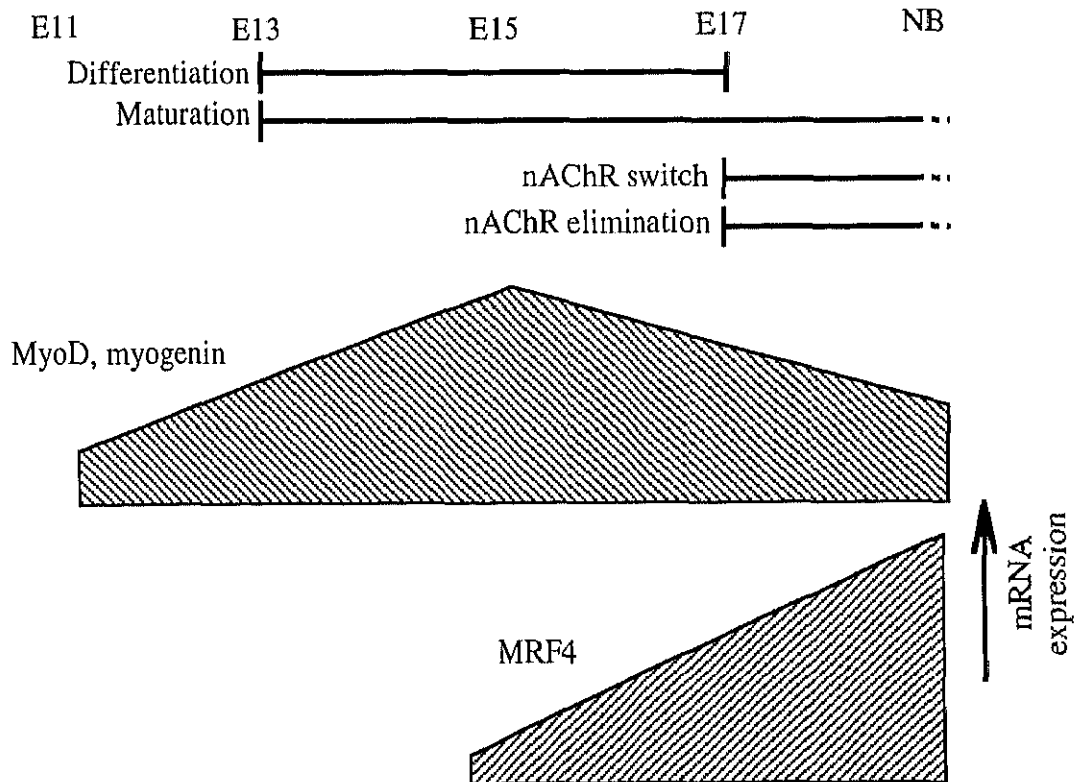


**Figure 13.**

**Electrophoretic gel pattern of IGF-I cDNA standard and its competitor (upper panel) after competitive PCR and the standard curve (lower panel).**

The standard curve in the lower panel was generated from the result of image analysis of electrophoretic bands in the upper panel. The formula of the regression line is represented by  $y = 0.46x - 0.15$ , where  $y$  is the logarithmic value of the ratio of the fluorescent intensity in the IGF-I cDNA standard band to that in its competitor band and  $x$  is the logarithmic value of the concentration of the cDNA standard. St. conc.; Standard concentrations. MW; molecular weight markers. bp; base pairs.

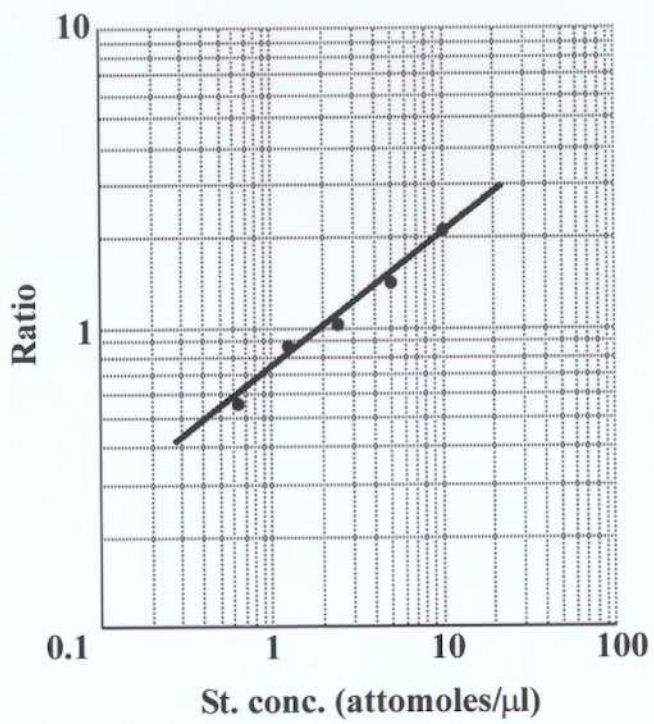
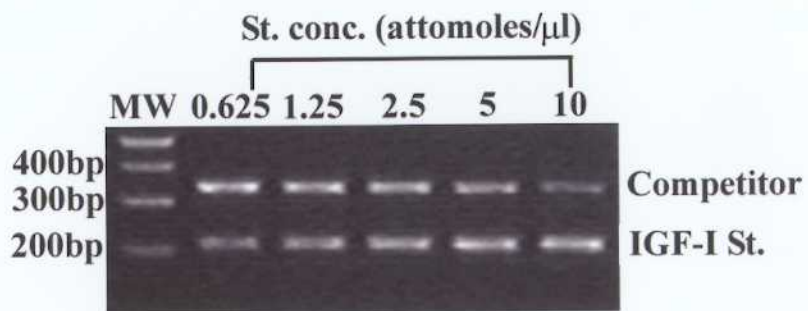


**Figure 14.**

**Changes in the relative amounts of IGF-I (A), II (B), IGFR 1 (C) and IGFR 2 (D) mRNAs in mouse tongues at stages E11, 13, 15 and 17, and at birth assessed by using competitive RT-PCR.**

Each point with its vertical bar represents the mean  $\pm$  1 SD of five or six samples. The vertical axis is expressed as a percentage of the mean value at the newborn stage. All the four mRNAs studied were highly expressed between E13 and E15 during which differentiation of myoblasts and formation of myotubes actively occurred. NB, newborn.

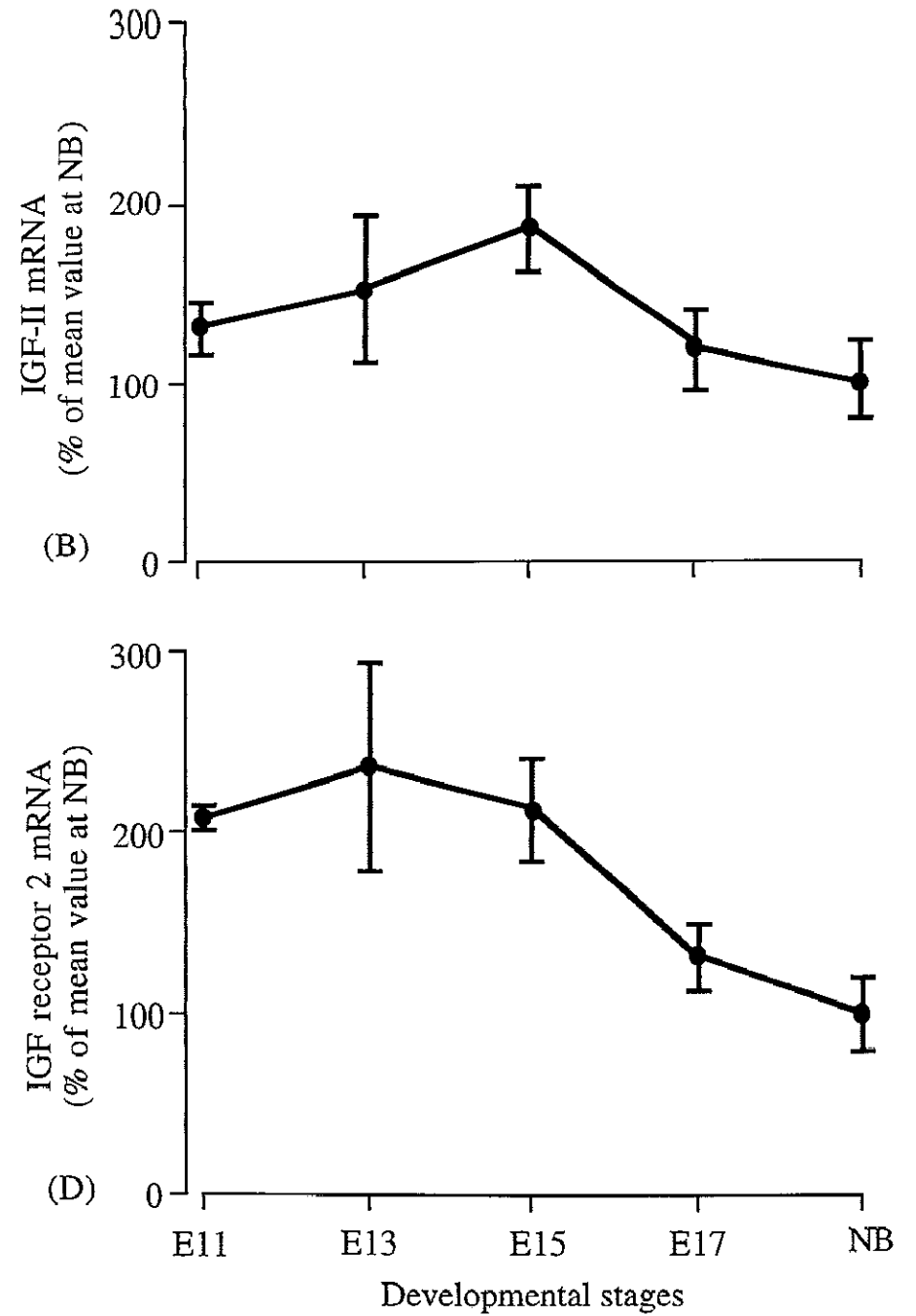
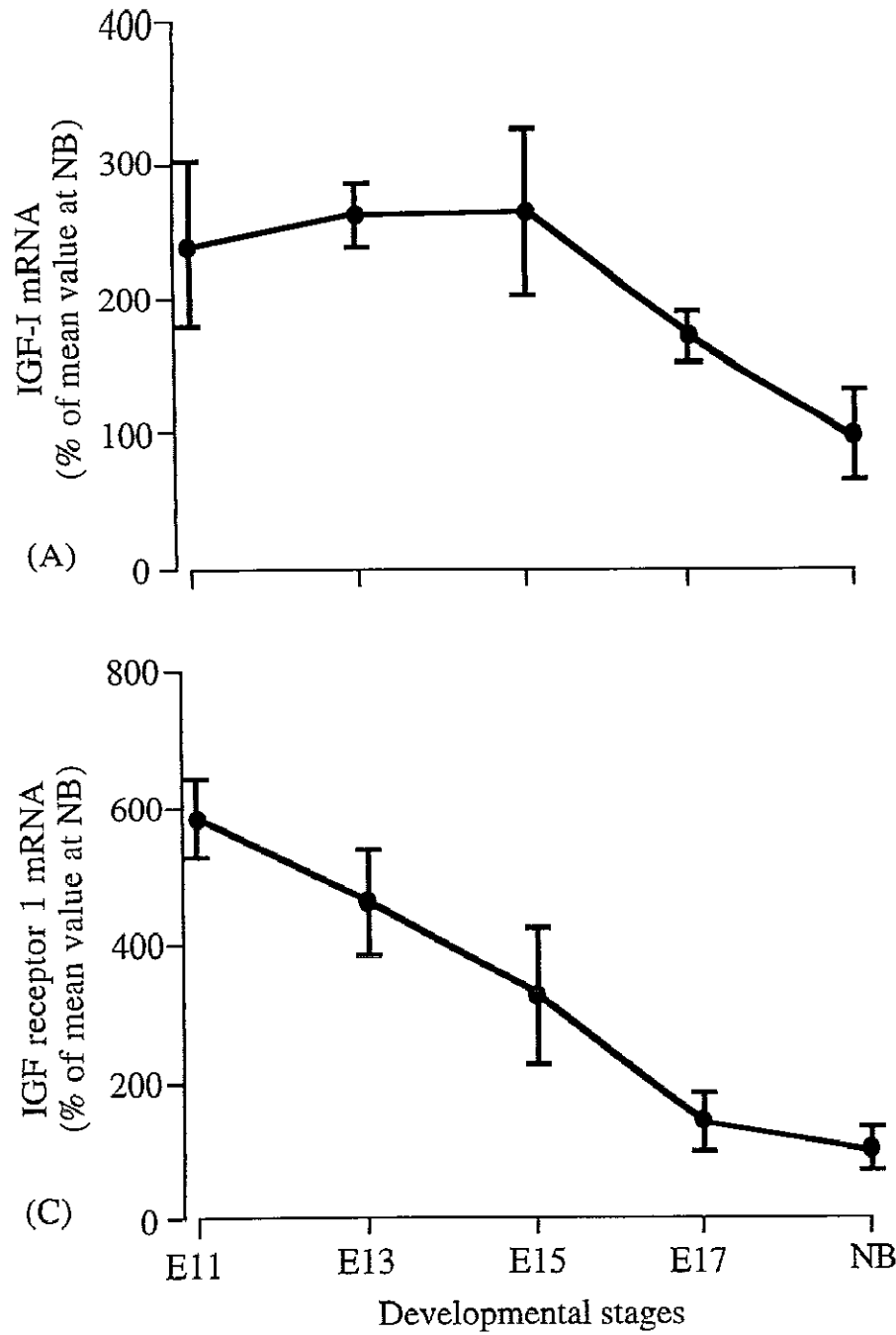


**Figure 15.**

**Confocal microscopic images of sagittal sections of tongues obtained from E13 (A, B, C) and E15 (D, E, F) mouse embryos, and newborn mice (G, H, I).**

A, D and G show immunostaining for IGF-I; C, F and I show immunostaining for fast myosin heavy chain; B, E and H show double-staining. Immunostaining for IGF-I was observed in differentiating myoblasts, myotubes and myofibers. The epithelial tissue (ep) displayed strong immunostaining for IGF-I at E15 (D) and newborn (G) stages. The top diagrammatic representation shows a sagittal section of tongue viewed from the buccal side. The squares indicate the regions shown in A ~ I.

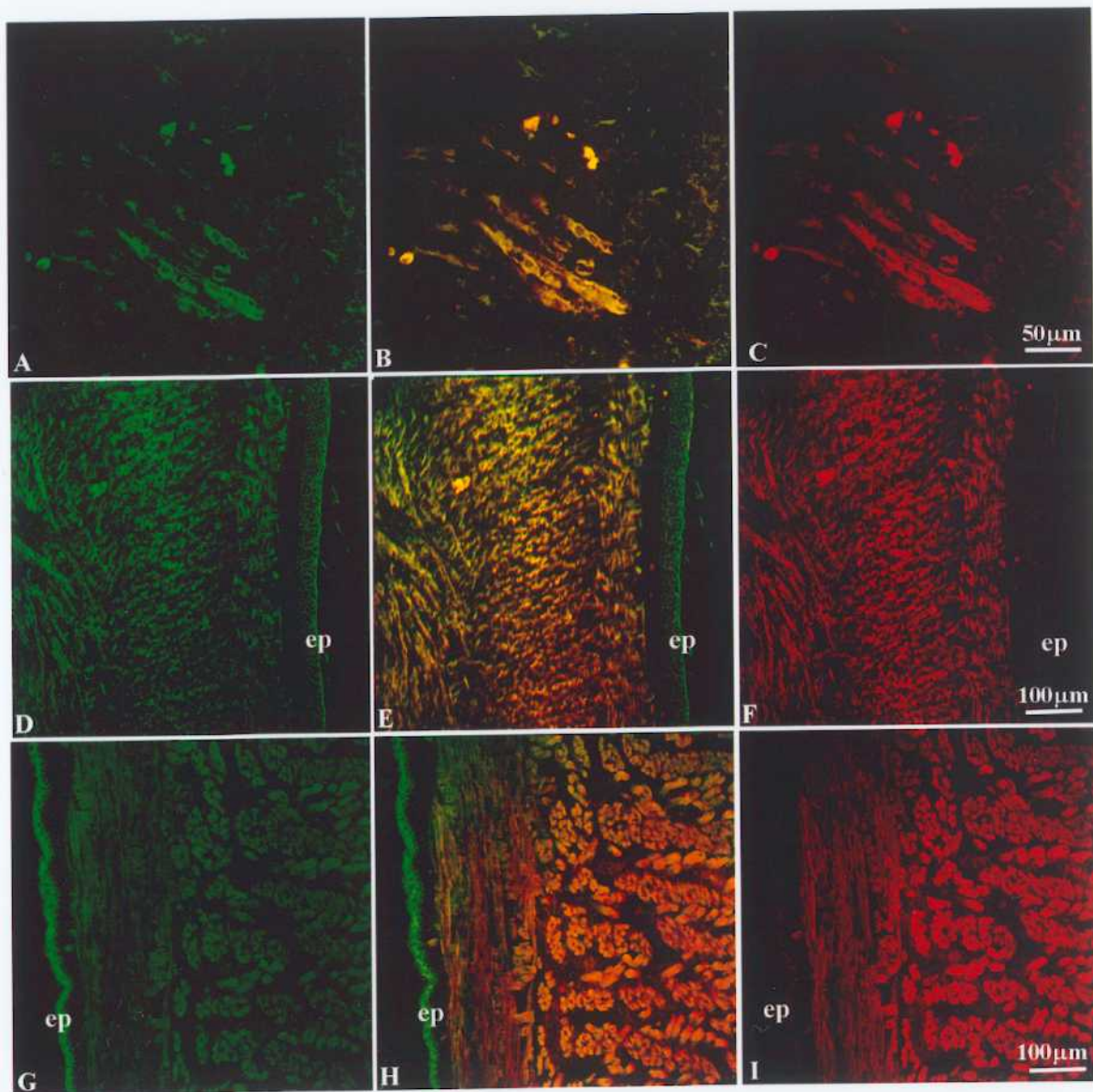
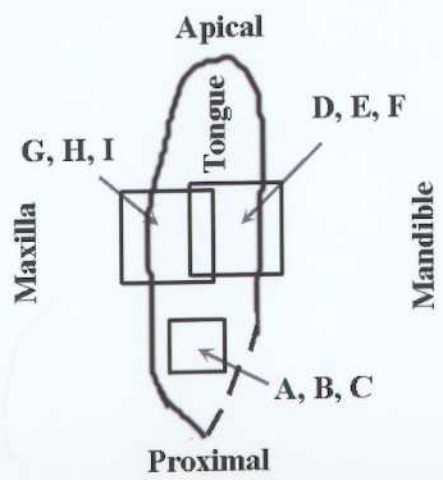


**Figure 16.**

**Confocal microscopic images of sagittal sections of tongues obtained from E13 (A, B, C) and E15 (D, E, F) mouse embryos, and newborn mice (G, H, I).**

A, D and G show immunostaining for IGF-II; C, F and I show immunostaining for fast myosin heavy chain; B, E and H show double-staining. Differentiating myoblasts, myotubes and myofibers were immunostained for IGF-II. The epithelial tissue (ep) displayed strong immunostaining for IGF-II at E15 (D) and newborn (G) stages. The top diagrammatic representation shows a sagittal section of tongue viewed from the buccal side. The squares indicate the regions shown in A ~ I.

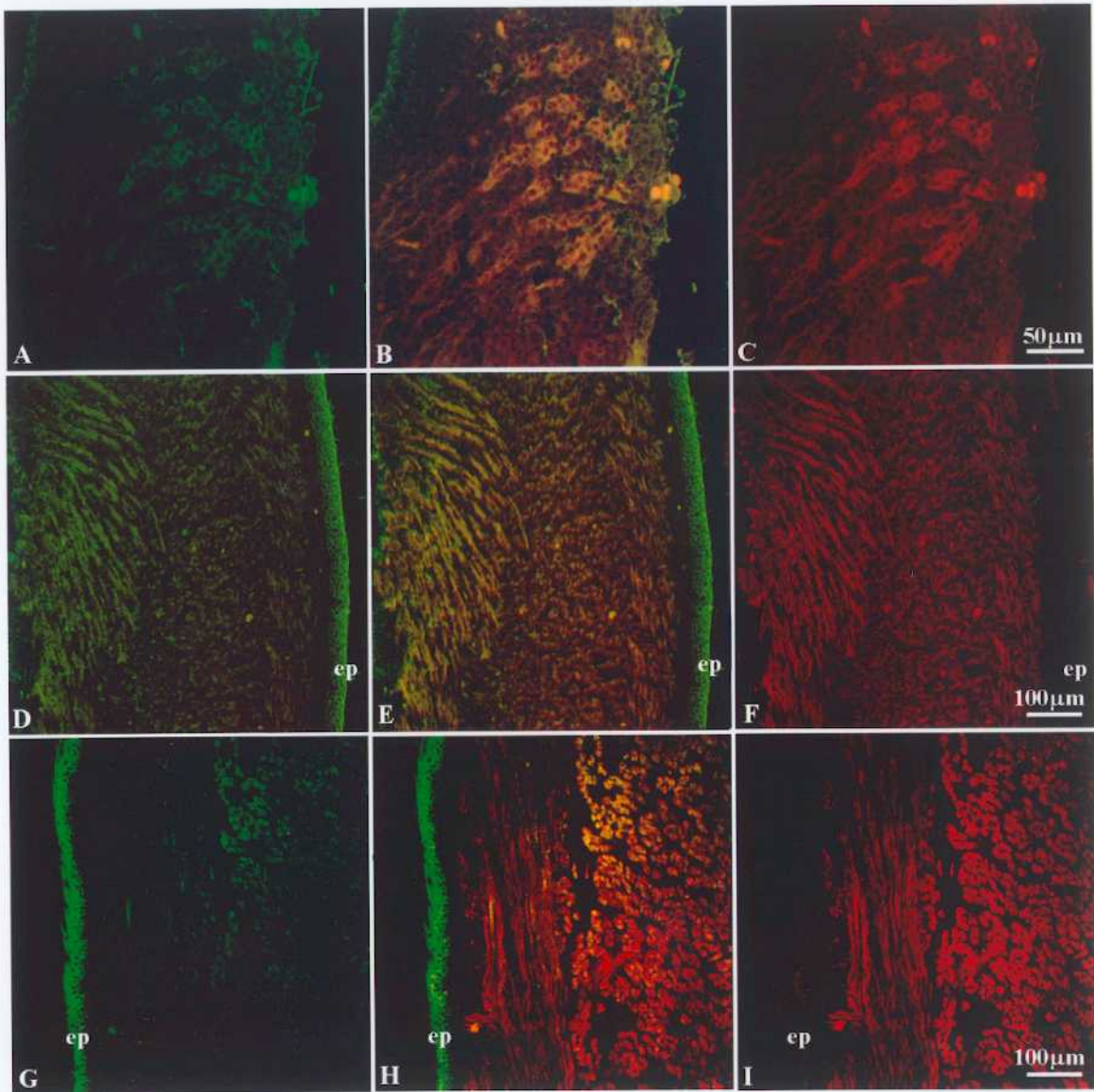
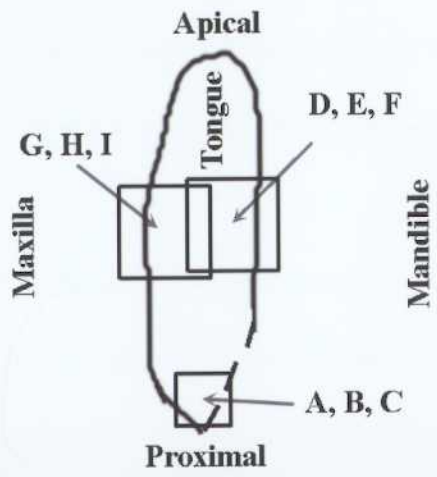


**Figure 17.**

**Confocal microscopic images of sagittal sections of tongues obtained from E13 (A, B, C) and E15 (D, E, F) mouse embryos, and newborn mice (G, H, I).**

A, D and G show immunostaining for IGFR 1; C, F and I show immunostaining for fast myosin heavy chain; B, E and H show double-staining. Immunostaining for IGFR 1 was also observed in differentiating myoblasts, myotubes and myofibers. ep, epithelial tissue. The top diagrammatic representation shows a sagittal section of tongue viewed from the buccal side. The squares indicate the regions shown in A ~ I.

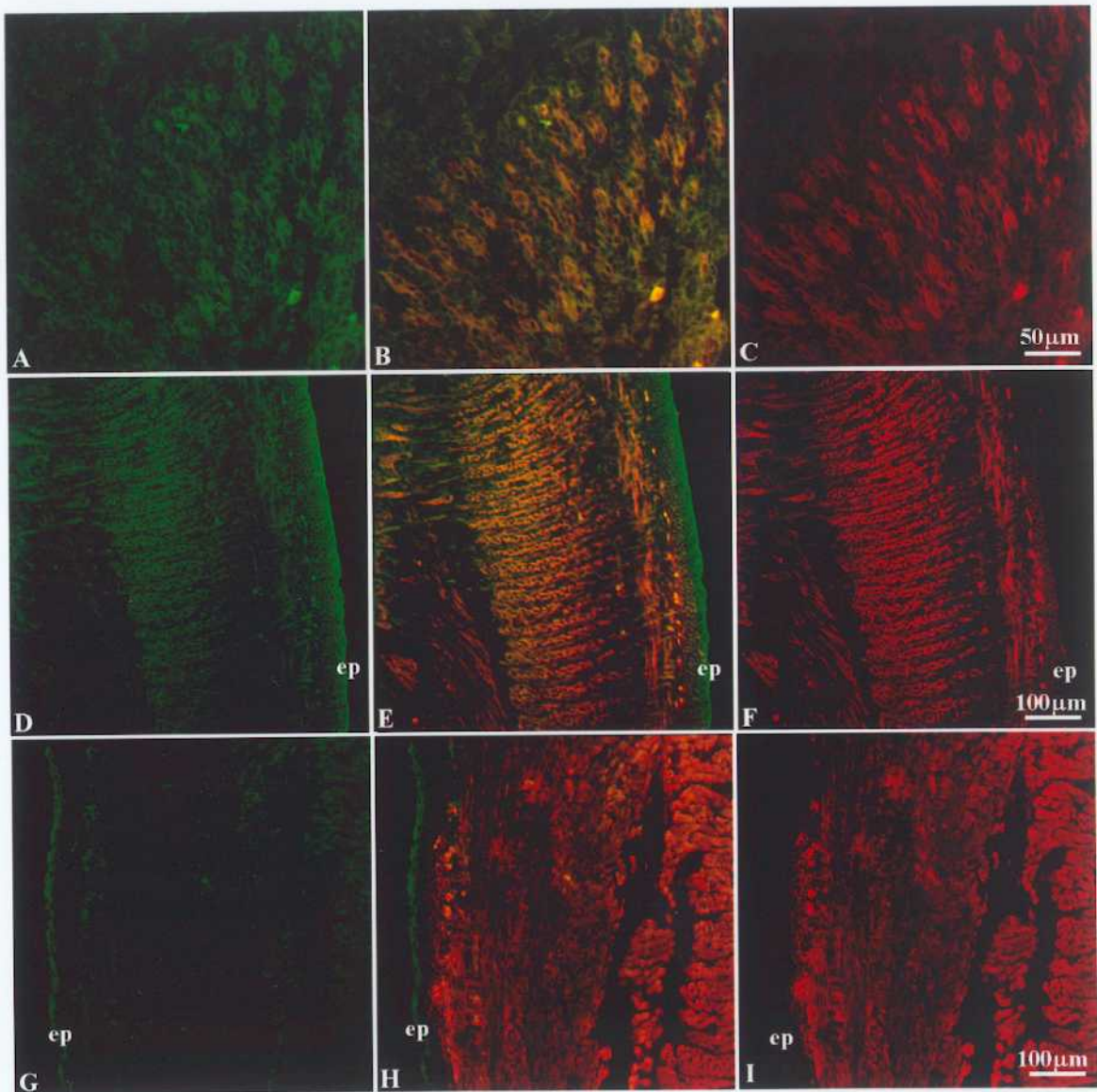
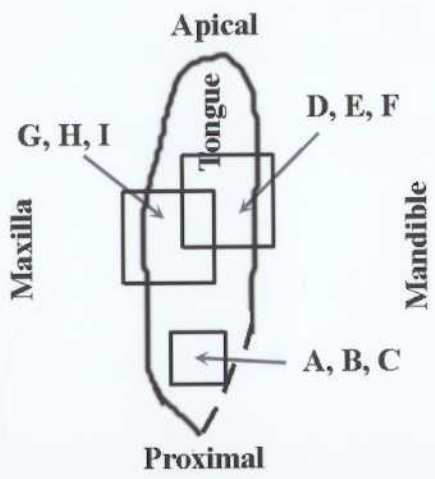


**Figure 18.**

**Confocal microscopic images of sagittal sections of tongues obtained from E13 (A, B, C) and E15 (D, E, F) mouse embryos, and newborn mice (G, H, I).**

A, D and G show immunostaining for IGFR 2; C, F and I show immunostaining for fast myosin heavy chain; B, E and H show double-staining. Immunostaining for IGFR 2 was sparsely distributed in the whole tongue and not restricted to differentiating striated muscle. ep, epithelial tissue. The top diagrammatic representation shows a sagittal section of tongue viewed from the buccal side. The squares indicate the regions shown in A ~ I.

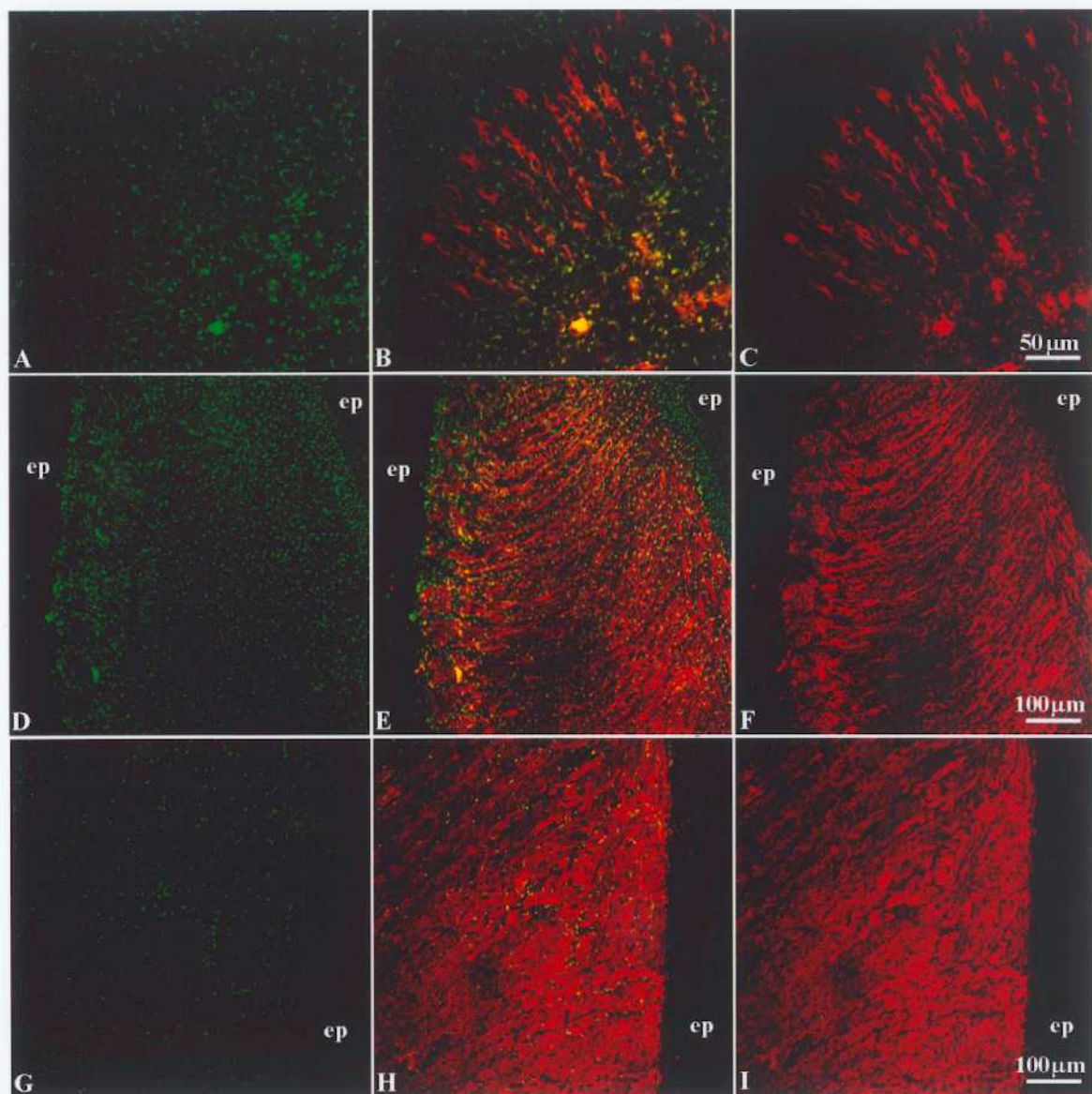
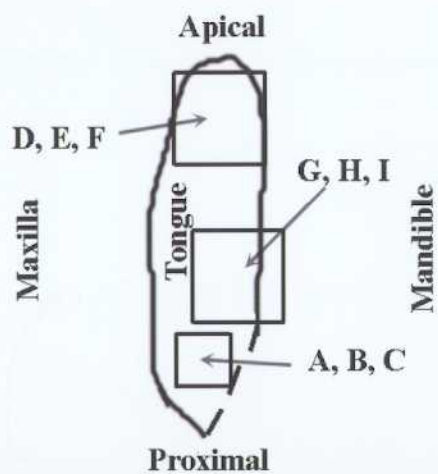
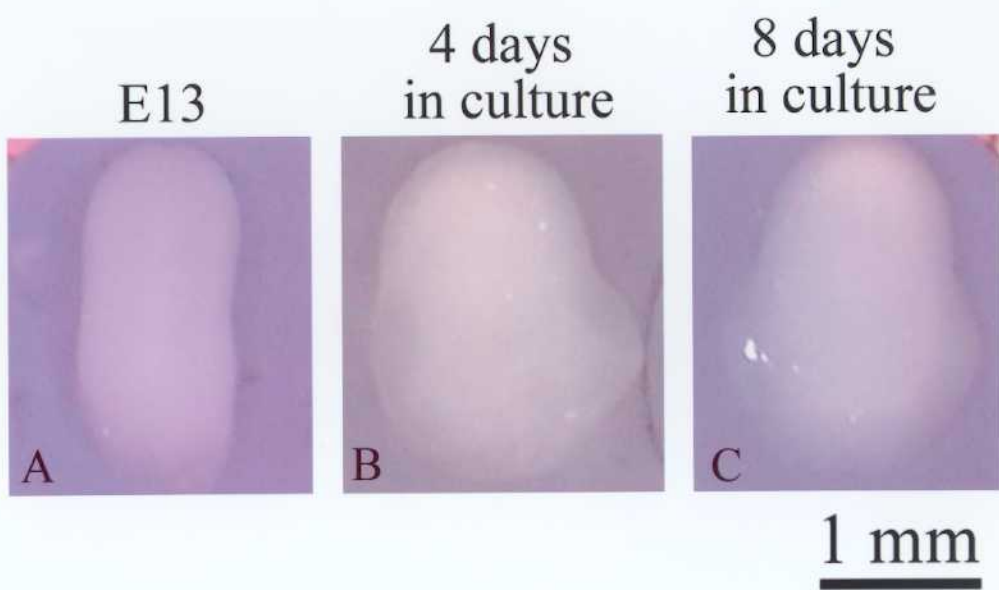


Figure 19.

A tongue dissected from E13 mouse embryos (A) and a tongue cultured for 4 (B) or 8 (C) days in BGJb medium.

The tongues appear to become round after 4 and 8 days in culture.



**Figure 20.**

**(A) Changes in the relative amount of muscle creatine kinase mRNA in the E13 tongues cultured for 0, 4 and 8 days assessed by using competitive RT-PCR.**

The content of muscle creatine kinase increased by 70 % between 0 and 4 days in culture. MCK, muscle creatine kinase.

**(B) Immunolocalization for fast myosin heavy chain in the proximal portions of E13 tongues cultured for 0, 4 and 8 days.**

In the proximal portion of E13 tongue, a few fast myosin heavy chain positive-myoblasts and myotubes were observed . After 4 days in culture, the number of fast myosin heavy chain positive-myoblasts and myotubes appears to increase. After 8 days in culture, several elongated myotubes were observed.

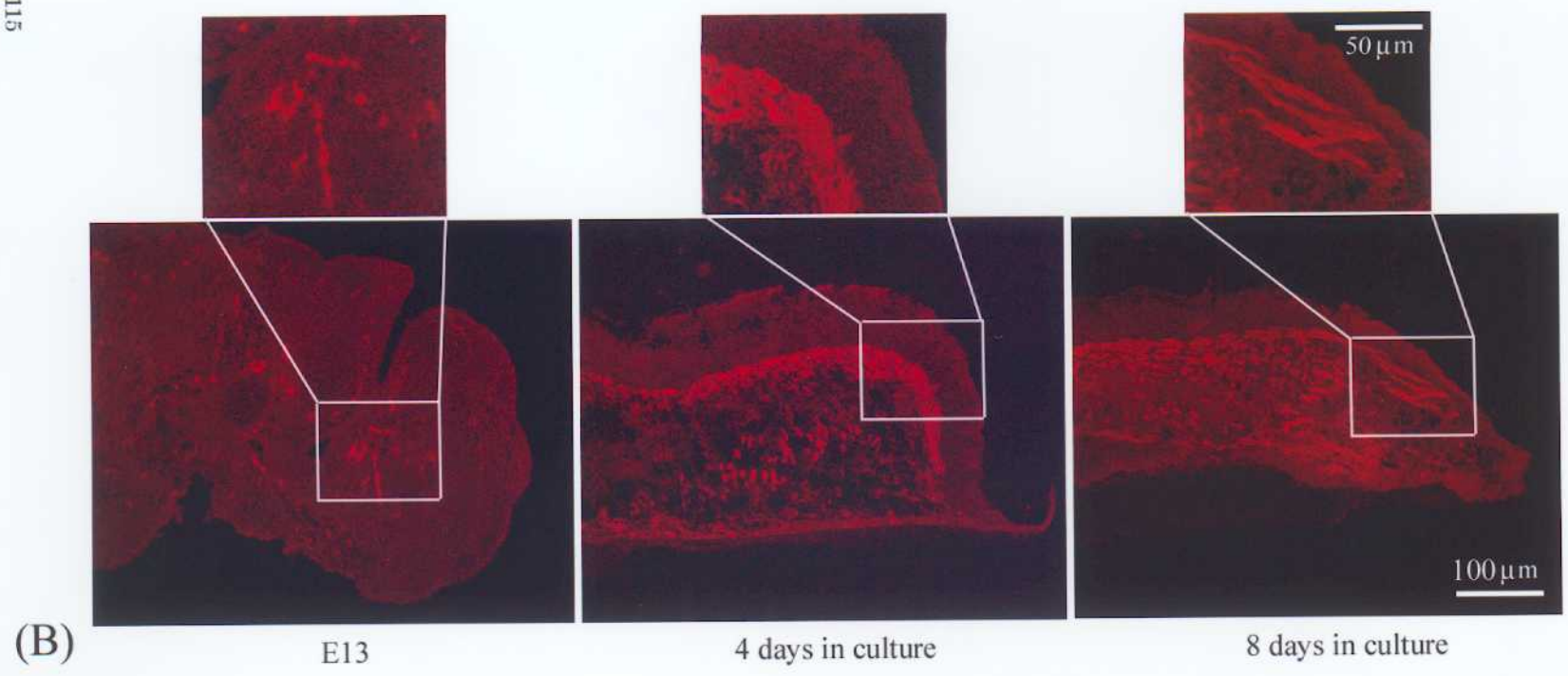
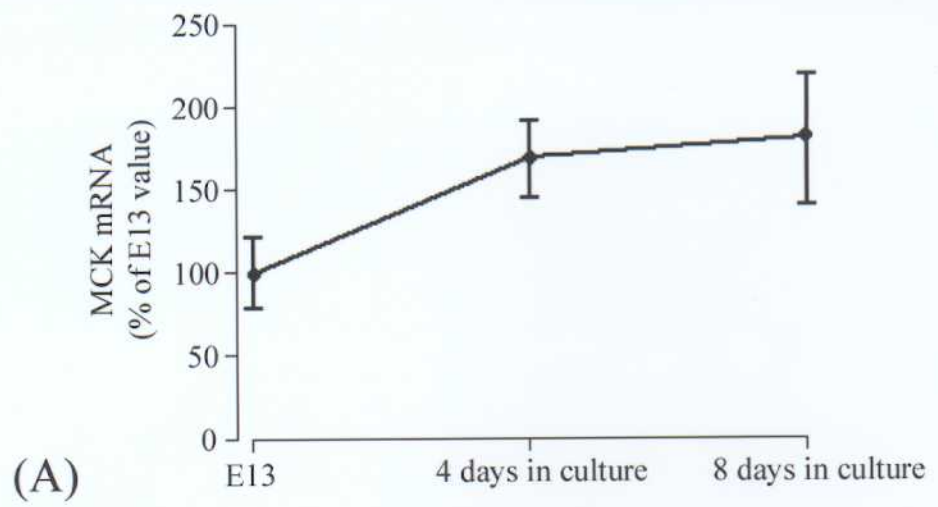
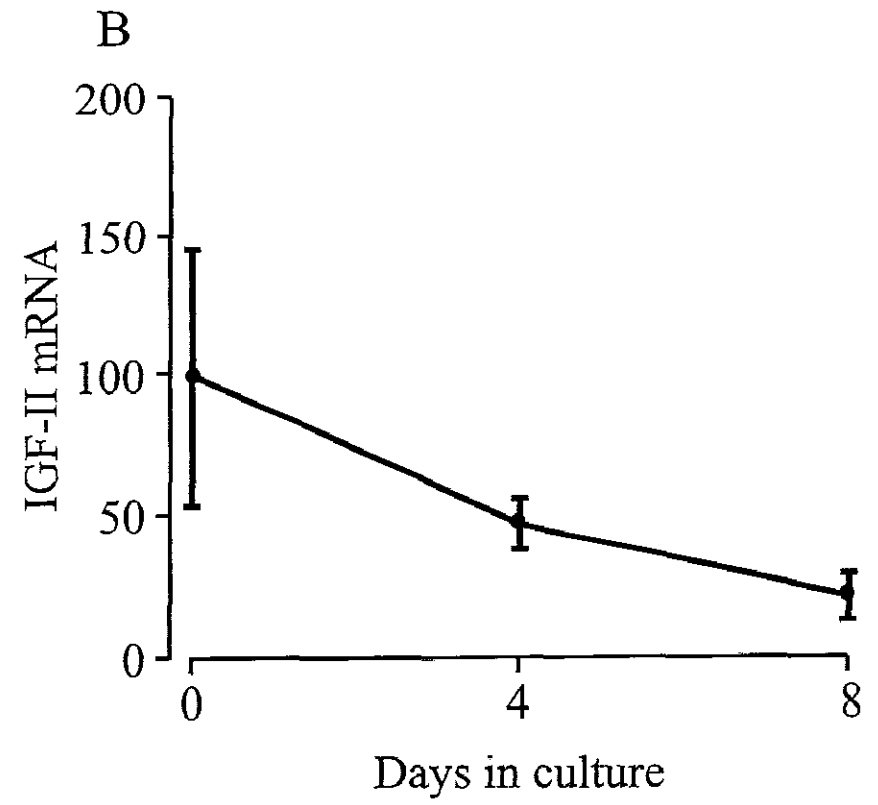
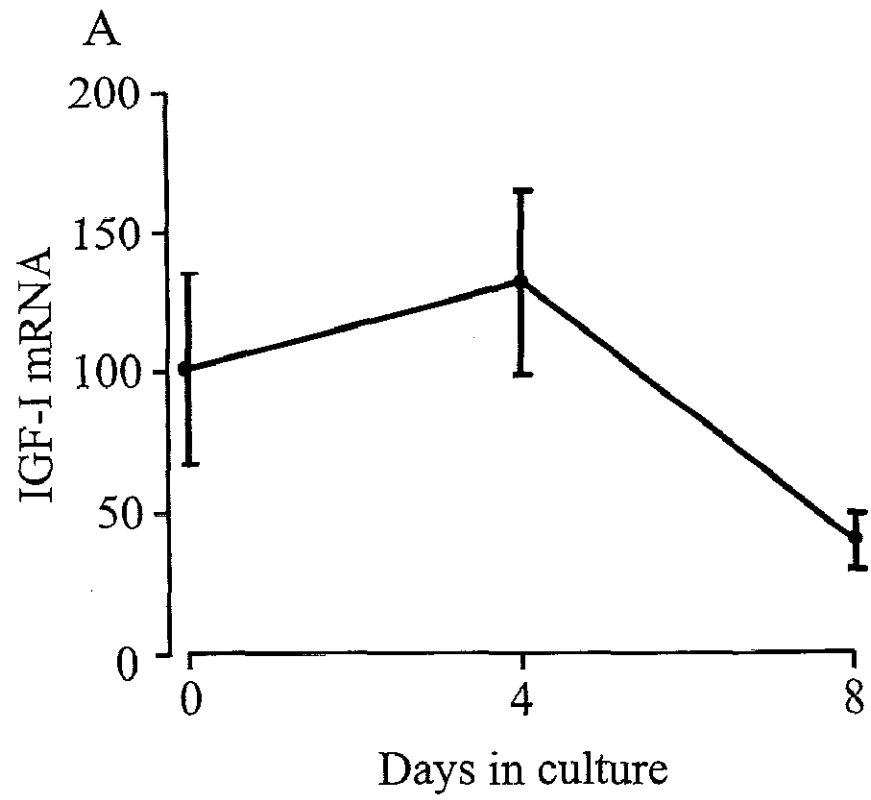


Figure 21.

Changes in the relative amounts of IGF-I (A) and IGF-II (B) mRNAs in the E13 tongues cultured for 0, 4 and 8 days assessed by using competitive RT-PCR.

IGF-I mRNA was highly expressed for the first 4 days of the culture period during which the myoblast differentiation actively occurs. IGF-II mRNA decreased in content throughout the whole culture period.



**Figure 22.**

**E13 tongues cultured in BGJb medium containing 0 (A), 25 (B), 50 (C) or 100 (D) ng/ml of IGF-I.**

No marked change in the shape and size was found between the control tongue cultured without IGF-I and the tongues cultured with IGF-I.

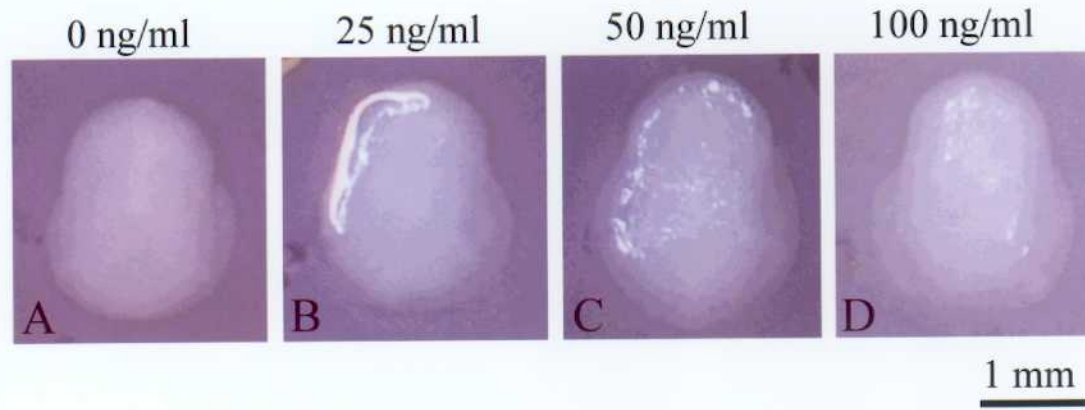


**Figure 23.**

**Changes in the relative amount of muscle creatine kinase (MCK) mRNA in the E13 tongues cultured in BGJb medium containing 0, 25, 50 or 100 ng/ml of IGF-I assessed by using competitive RT-PCR.**

The treatment of 50 ng/ml IGF-I induced a 30 % ( $p < 0.01$ ) increase in the mRNA content of muscle creatine kinase.

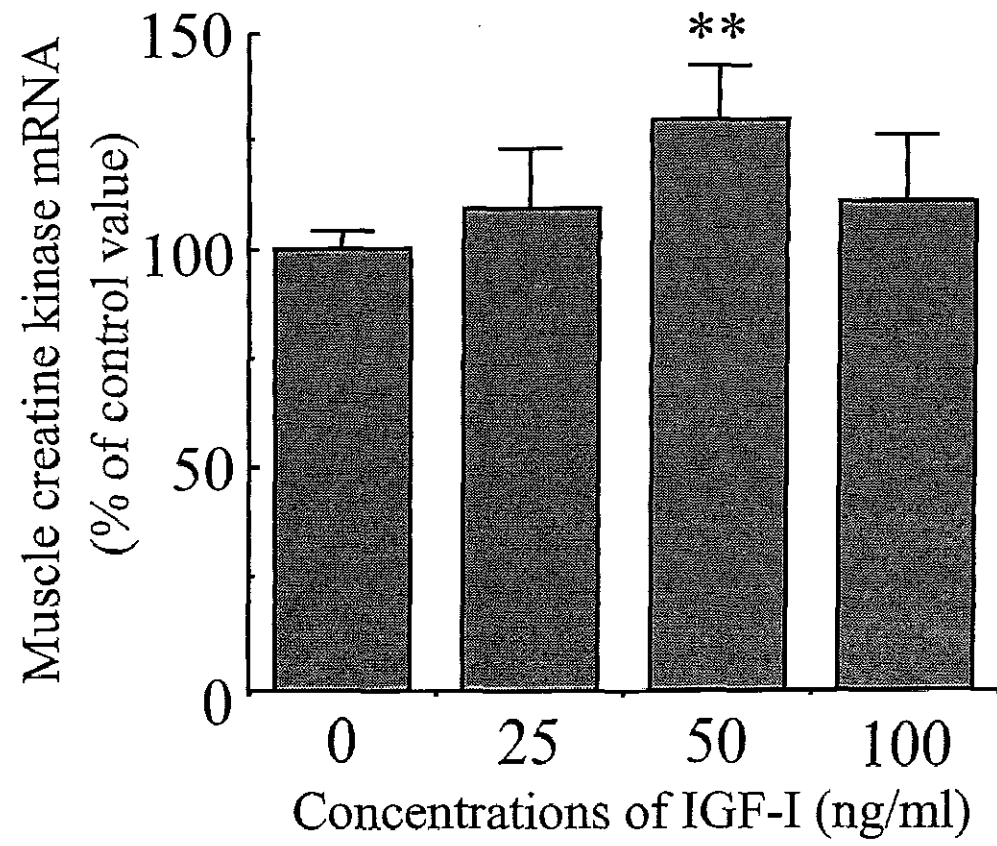


**Figure 24.**

**Changes in the relative amounts of myf5 (A), myoD (B), myogenin (C) and MRF4 (D) mRNAs in the E13 tongues cultured in BGJb medium containing 0, 25, 50 or 100 ng/ml of IGF-I assessed by using competitive RT-PCR.**

The treatments with 50 and 100 ng/ml of IGF-I induced 35 % ( $p < 0.05$ ) and 41 % ( $p < 0.05$ ) increases in the mRNA contents of myogenin and myoD, respectively.

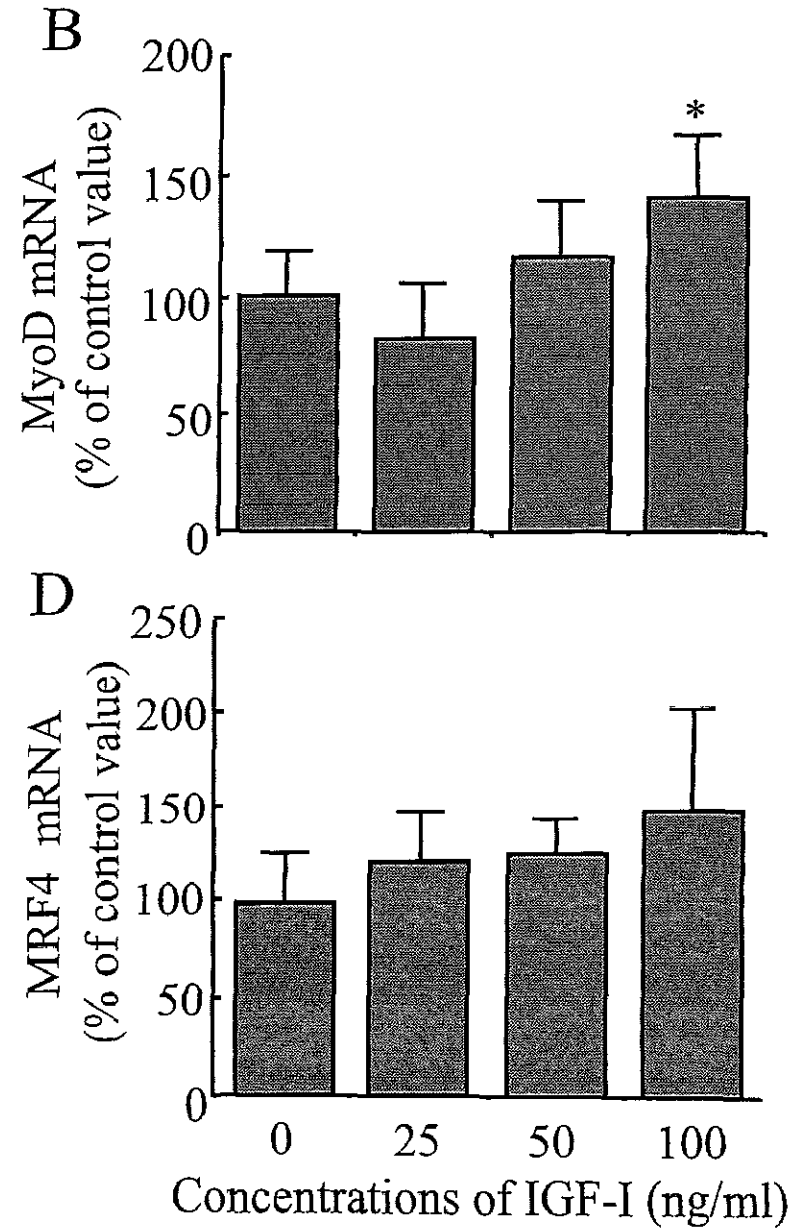
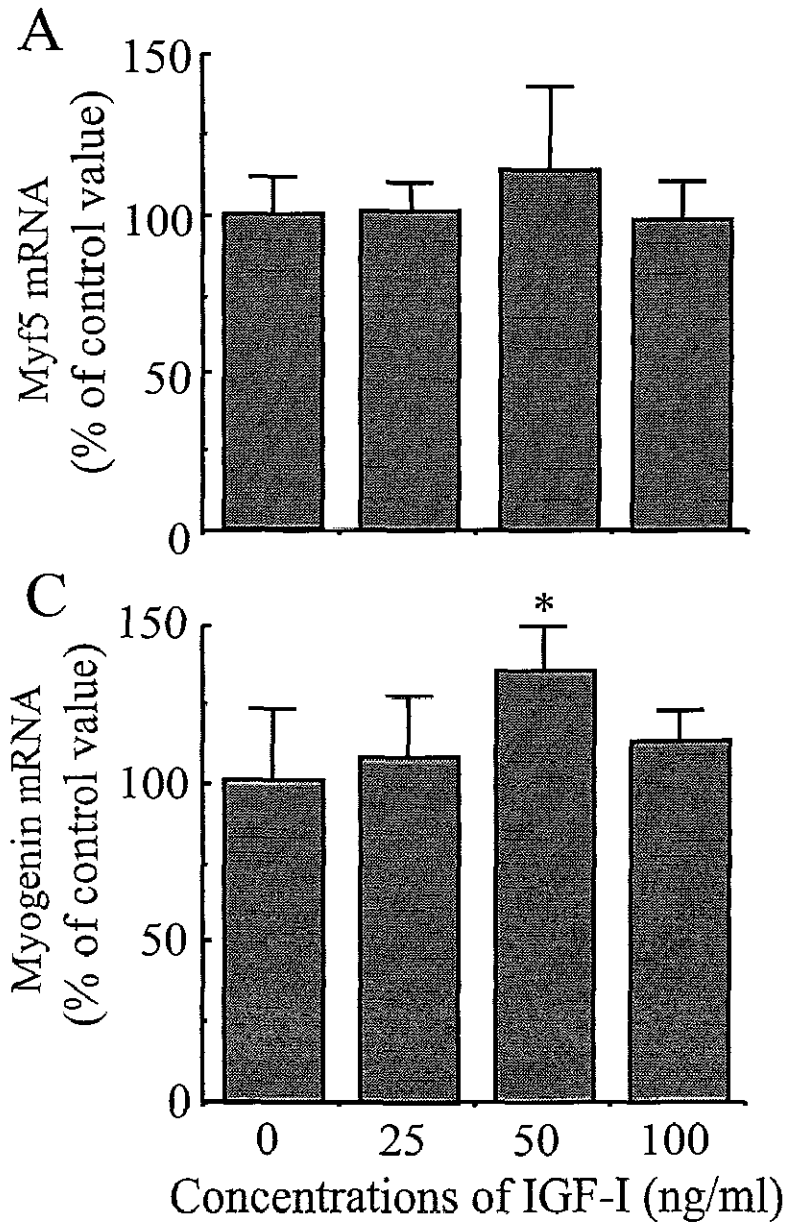
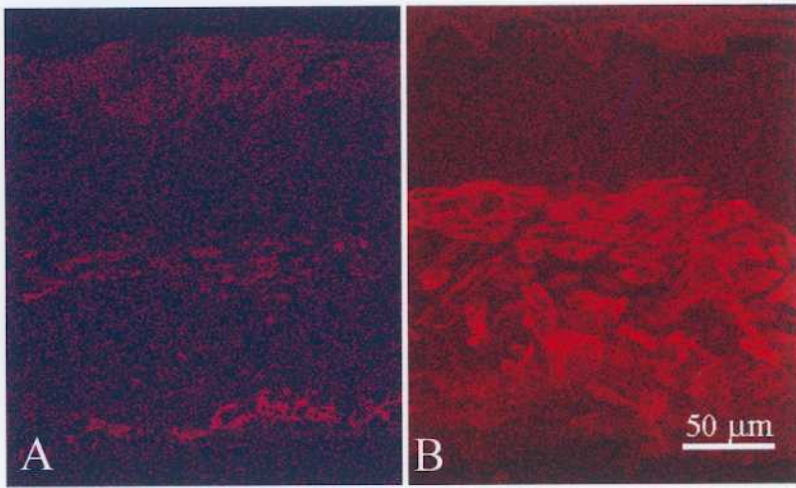


Figure 25.

Immunolocalization of fast myosin heavy chain in the middle portions of sagittal sections of tongues cultured without IGF-I (A) and with 50 ng/ml of IGF-I (B).

The treatment with 50 ng/ml of exogenous IGF-I appears to induce an increase in the number of fast myosin heavy chain-positive myoblasts and myotubes.



**Figure 26.**

**Changes in the relative amounts of IGFBP2 (A), 3 (B), 4 (C) , 5 (D) and 6 (E) mRNAs in the E13 tongues cultured in BGJb medium containing 0, 25, 50 or 100 ng/ml of IGF-I assessed by using competitive RT-PCR.**

No significant difference was found in the contents of exogenous IGFBP2 and 3 mRNAs. The treatments with 50 and 100 ng/ml of exogenous IGF-I induced approximately 50 ~ 60 % ( $p < 0.05 \sim 0.01$ ) increases in the contents of endogenous IGFBP4 and 5 mRNAs. Only the treatment with 100 ng/ml of exogenous IGF-I induced a 76 % ( $p < 0.05$ ) increase in the mRNA content of endogenous IGFBP6. IGFBP1 mRNA was not able to be detected by this PCR technique (data not shown).

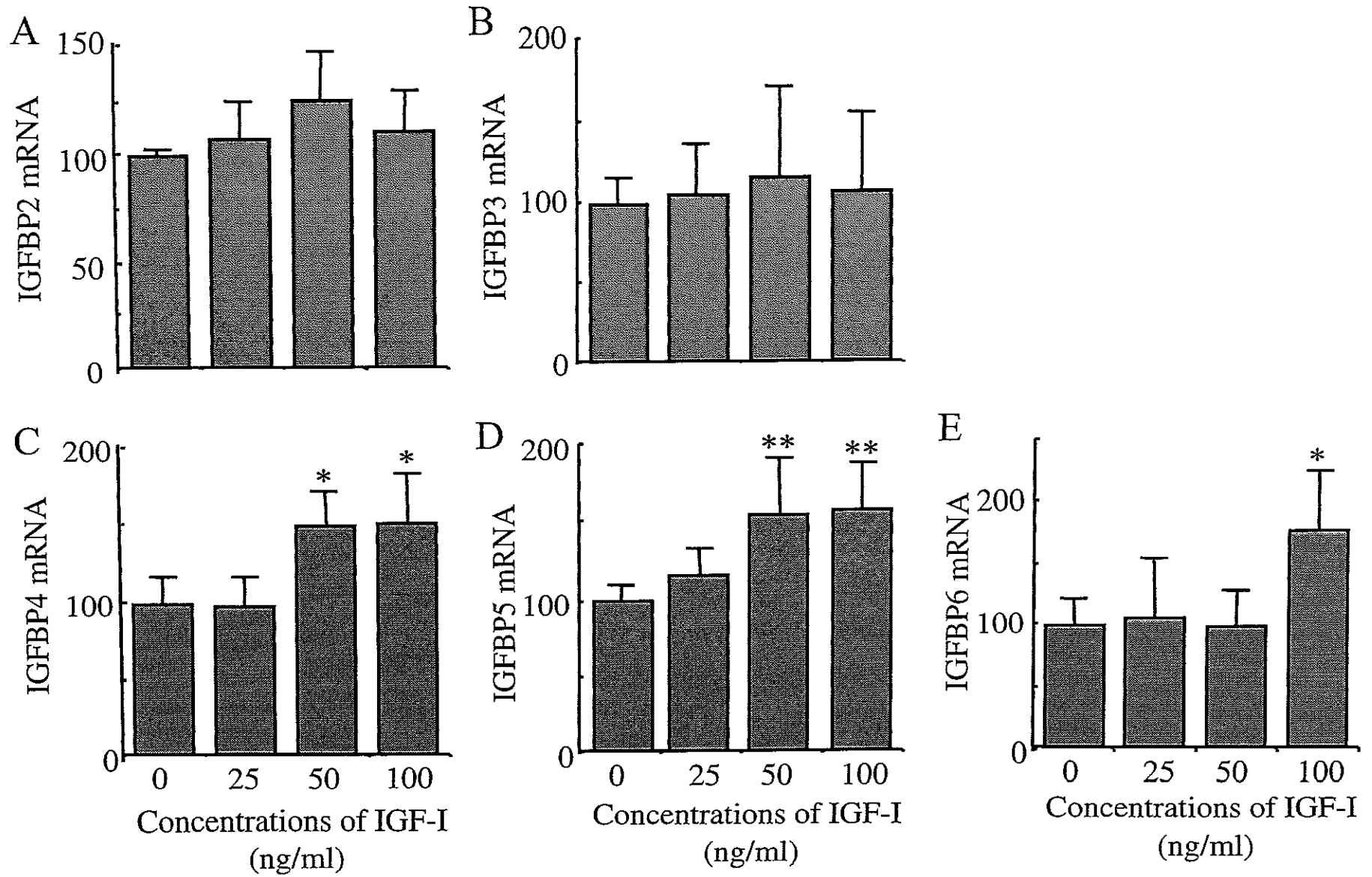


Figure 27.

Immunolocalization of insulin-like growth factor binding protein

(IGFBP) 4 (A, B), 5 (C, D) and 6 (E, F) in the middle portions of sagittal sections of tongues cultured without IGF-I (A, C, E) and with 50 ng/ml of IGF-I (B, D, F).

In the striated muscle tissues in the middle portion of the cultured tongue, intense immunostaining for IGFBP4 (A and B) and 5 (C and D) was observed. In the epithelium and the tissues underneath the epithelium, very intense staining for IGFBP6 was observed (E and F).

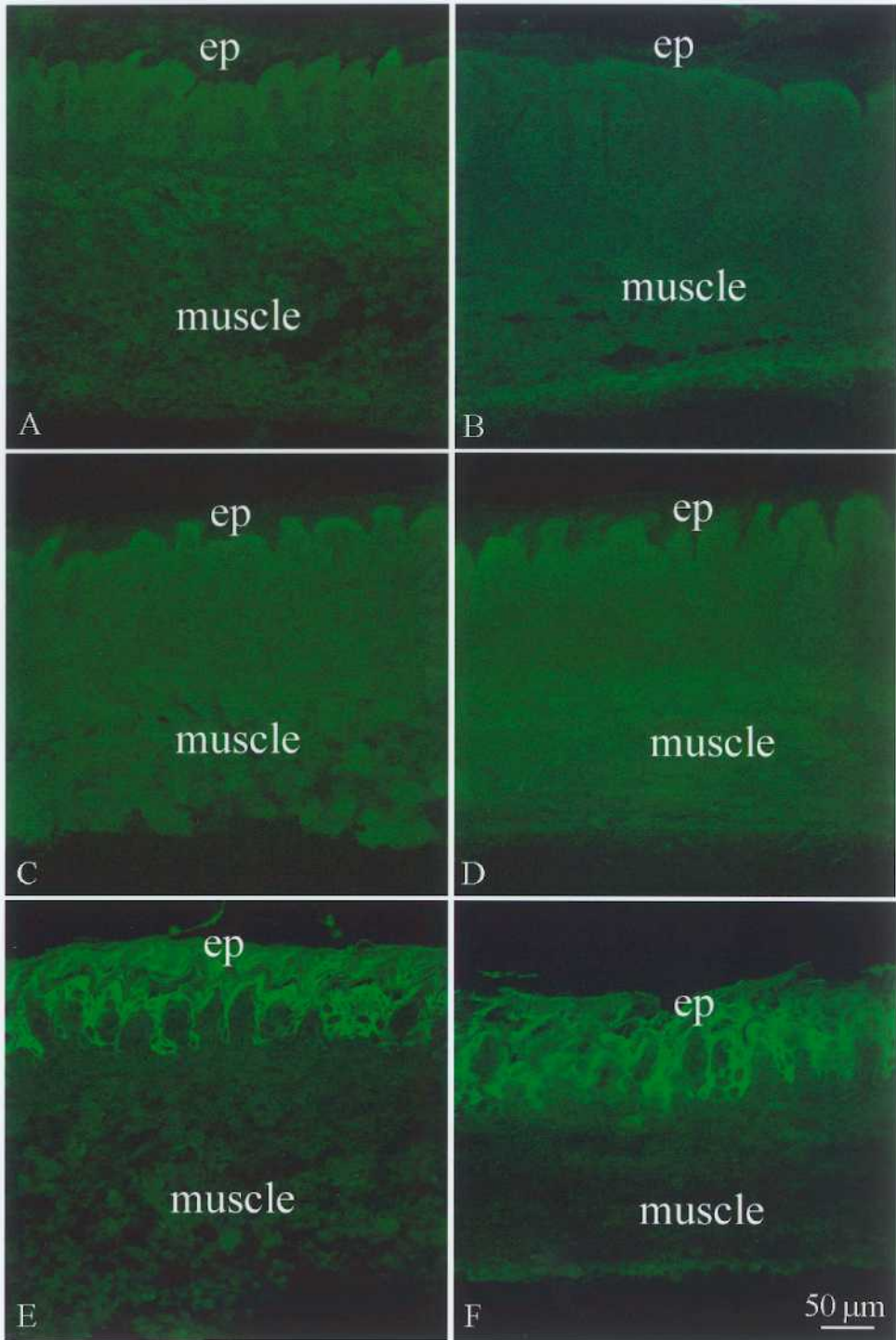


Figure 28.

Changes in the relative amounts of muscle creatine kinase (A) and myogenin (B) mRNAs in the E13 tongues cultured in BGJb medium containing 0, 100, 200 or 400 ng/ml of IGFBP4 assessed by using competitive RT-PCR.

The treatment with 200 ng/ml of exogenous IGFBP4 induced a 70 % ( $p < 0.01$ ) increase in the content of myogenin mRNA. MCK, muscle creatine kinase.

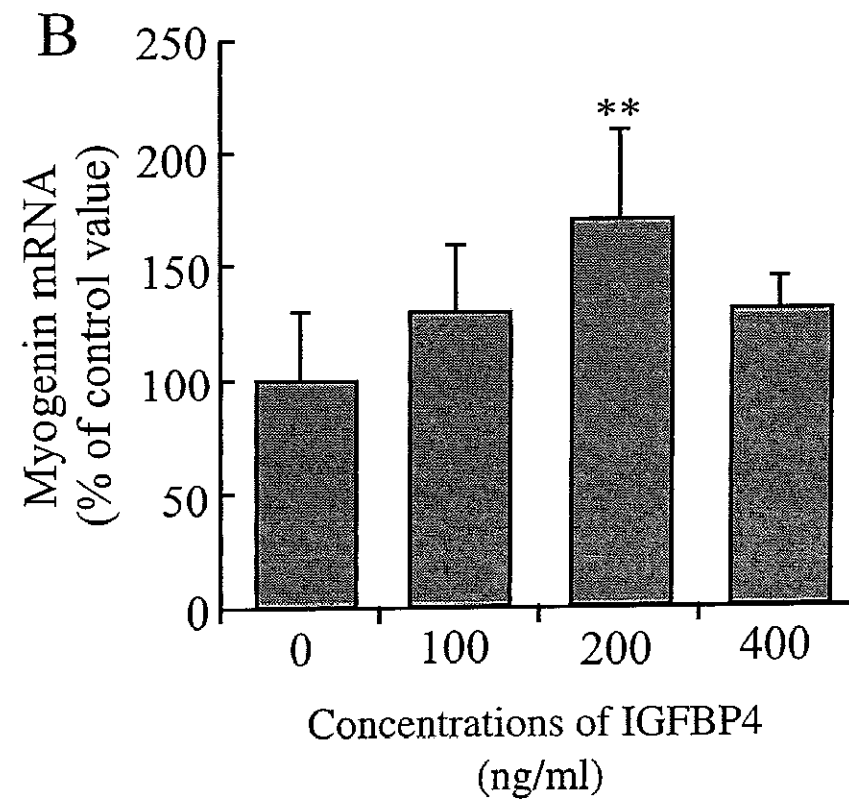
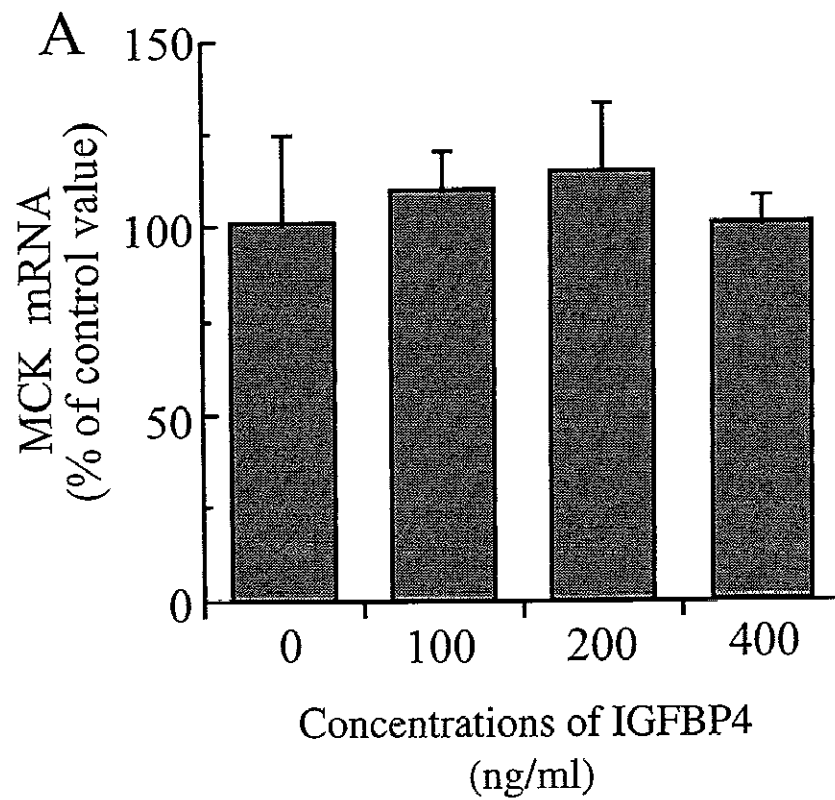
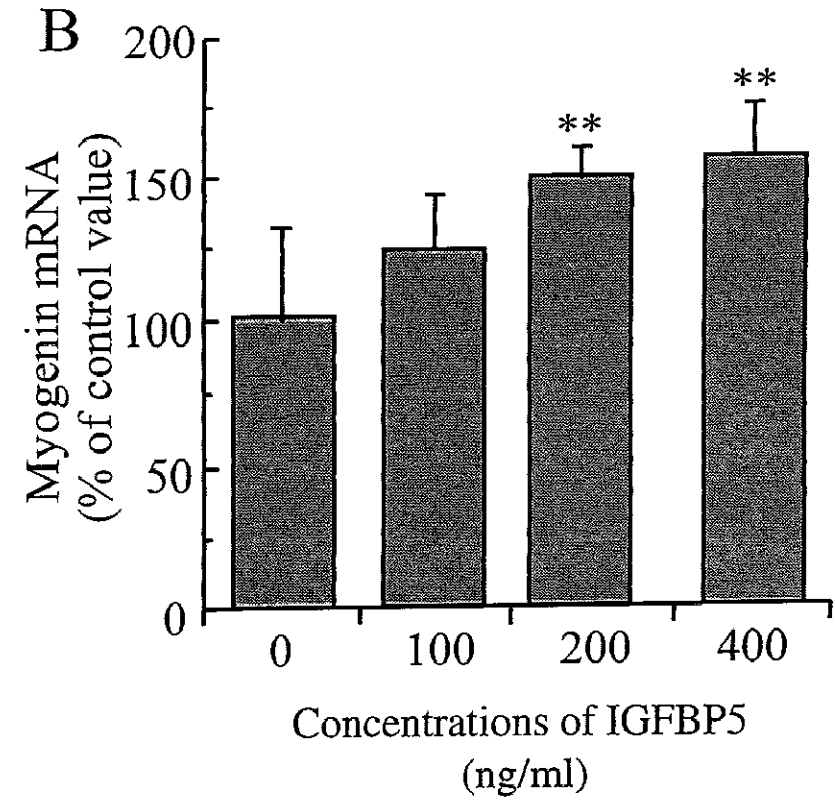
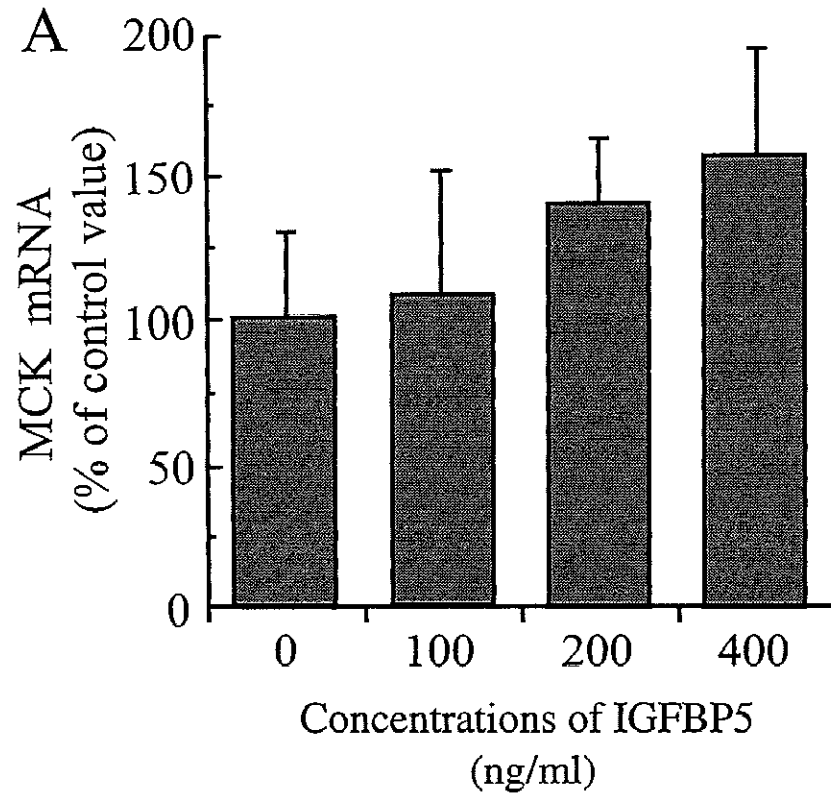


Figure 29.

Changes in the relative amounts of muscle creatine kinase (A) and myogenin (B) mRNAs in the E13 tongues cultured in BGJb medium containing 0, 100, 200 or 400 ng/ml of IGFBP5 assessed by using competitive RT-PCR.

The treatments with 200 and 400 ng/ml of exogenous IGFBP5 induced 49 % ( $p < 0.01$ ) and 55 % ( $p < 0.01$ ) increases in the myogenin mRNA expression, respectively.



**Figure 30.**

**Changes in the relative amounts of muscle creatine kinase (A) and myogenin (B) mRNAs in the E13 tongues cultured in BGJb medium containing 0, 100, 200 or 400 ng/ml of IGFBP6 assessed by using competitive RT-PCR.**

IGFBP6 did not induce any significant changes in the contents of muscle creatine kinase and myogenin mRNAs. MCK, muscle creatine kinase.

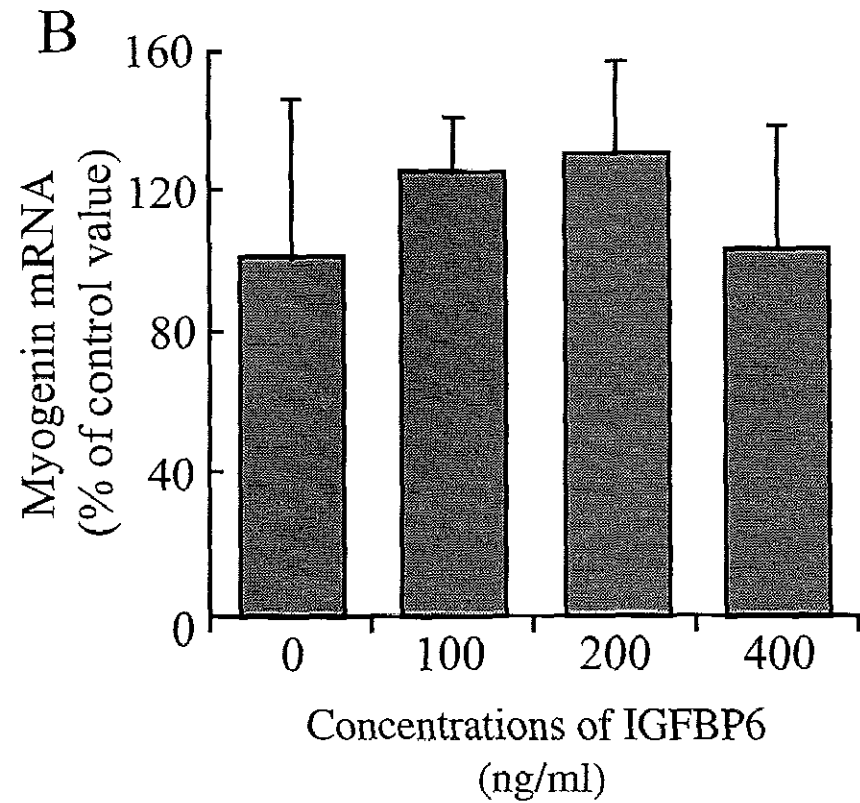
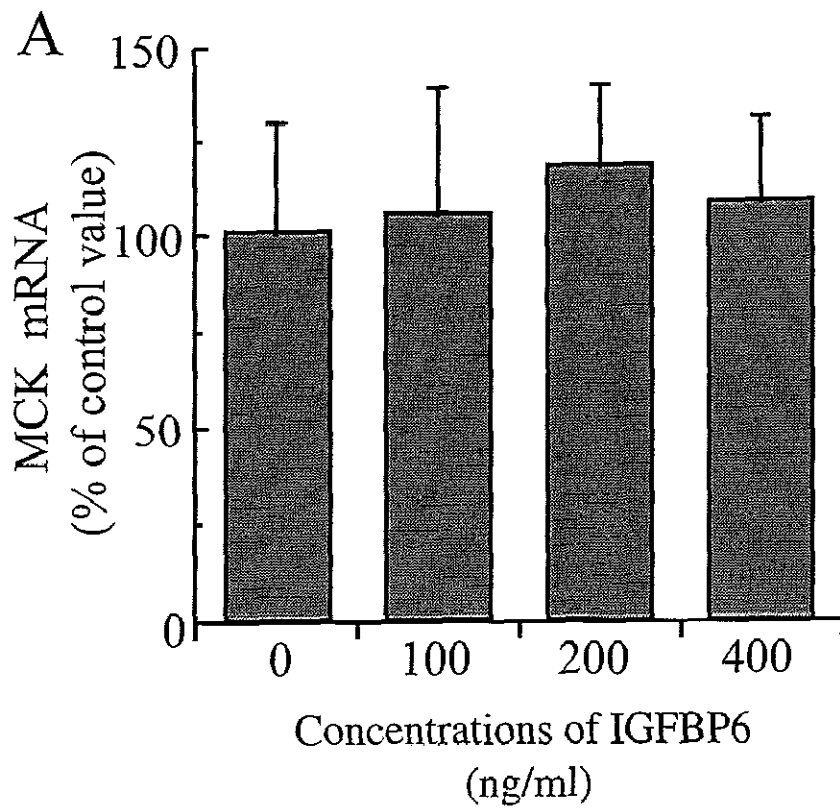
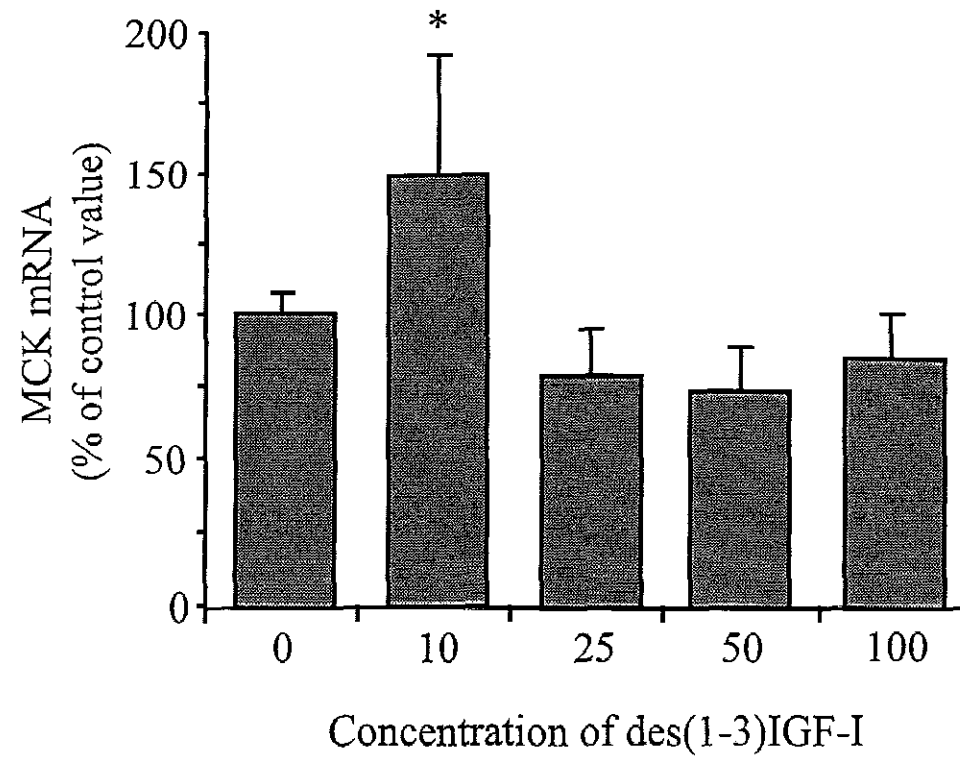


Figure 31.

Changes in the relative amount of muscle creatine kinase (MCK) mRNA in the E13 tongues cultured in BGJb medium containing 0, 10, 25, 50 or 100 ng/ml of des(1-3)IGF-I assessed by using competitive RT-PCR.

The treatment with 10 ng/ml des(1-3)IGF-I induced a 48 % ( $p < 0.05$ ) increase in the content of muscle creatine kinase mRNA.



**Figure 32.**

**Changes in the relative amounts of myf5 (A), myoD (B), myogenin (C) and MRF4 (D) mRNAs in the E13 tongues cultured in BGJb medium containing 0, 10, 25, 50 or 100 ng/ml of des(1-3)IGF-I assessed by using competitive RT-PCR.**

The treatments with 25~100 ng/ml of des(1-3)IGF-I induced 20~50% ( $p < 0.05 \sim 0.01$ ) decreases in the contents of myf5, myoD and myogenin mRNAs.

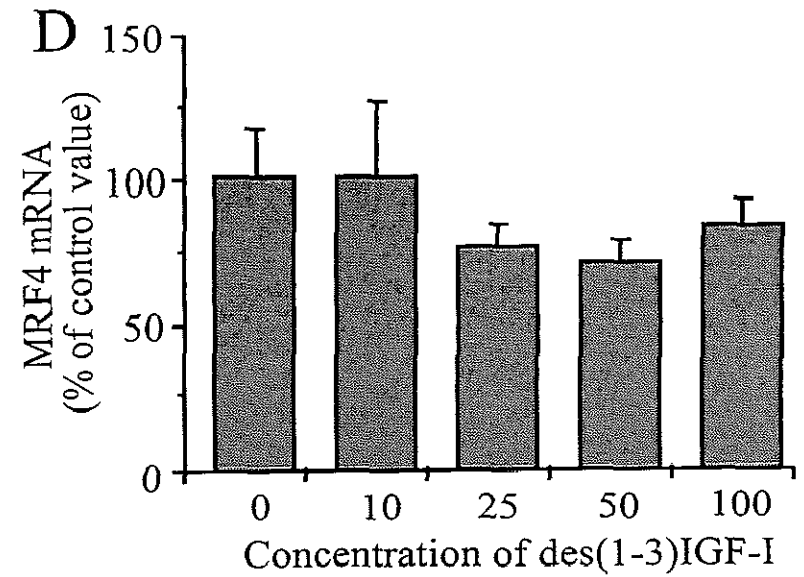
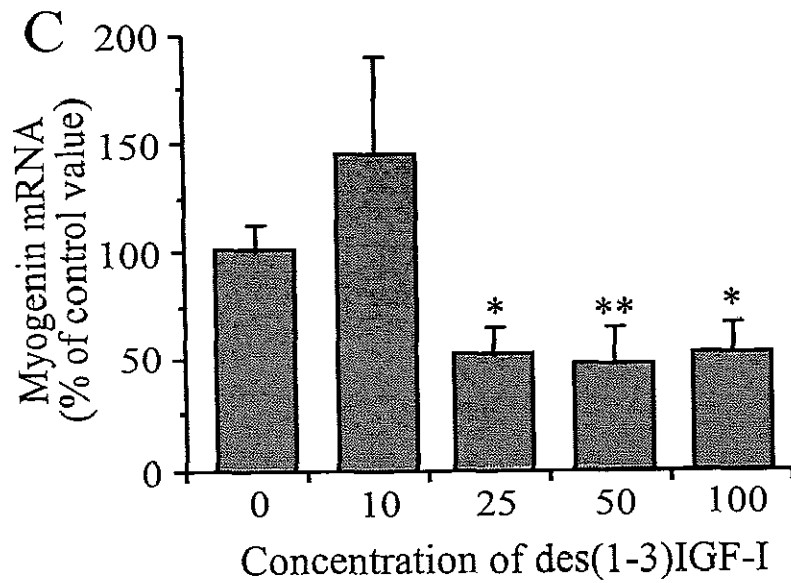
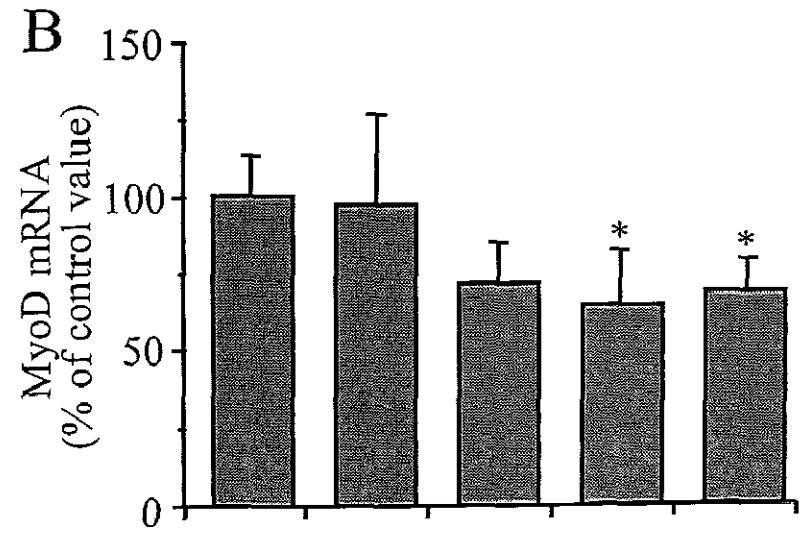
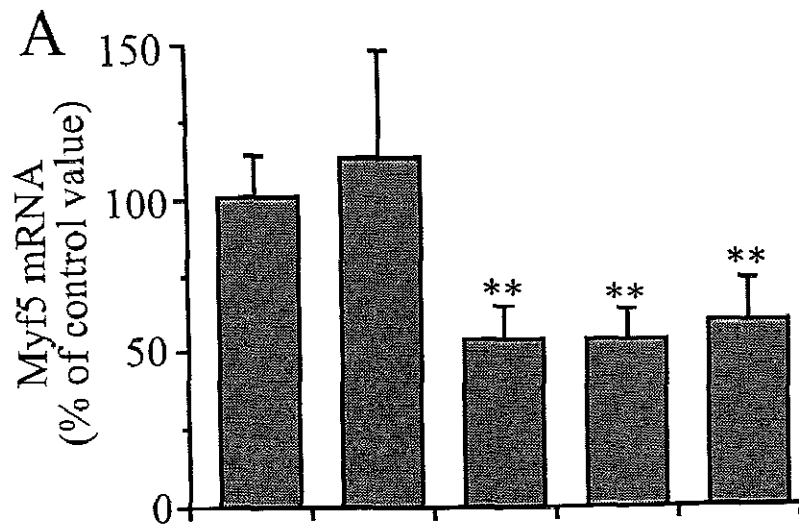


**Figure 33.**

**The tongues cultured with (A) or without 50 ng/ml des(1-3)IGF-I (B) and the middle portions in sagittal sections of the control (C) and des(1-3)IGF-I treated (D) tongues stained with by hematoxylin and eosin.**

The shape of tongue treated with des(1-3)IGF-I appears to be quite different from that of control tongue. Abnormal tissues were observed in the peripheral region of the tongue.

Staining intensity with hematoxylin and eosin, and cell density in the des(1-3)IGF-I treated tongue appear to be less in comparison with the control tongue. Arrows indicate multinucleated myotubes.

